**Table 1**
Selected test chemicals used in the validation study.

| No. | Chemical name | CAS No. | Photosafety information | | | UV absorption[a] | | ROS assay data[b] | | | | | | |
|---|---|---|---|---|---|---|---|---|---|---|---|---|---|---|
| | | | 3T3 NRU PT | Animal | Human | $\lambda_{max}$ (nm) | $\varepsilon \times 10^3$ ($M^{-1}cm^{-1}$) | Lab#1 | Lab#2 | Lab#3 | Lab#4 | Lab#5 | Lab#6 | Lab#7 |
| | | | | | | | | Suntest CPS (Atlas) | | | SXL-2500V2 (Seric) | | | |
| *Positive/negative controls* | | | | | | | | | | | | | | |
| 1 | Quinine HCl | 6119-47-7 | + | + | + | 330 | 1.9 | + | + | + | + | + | + | + |
| 2 | Sulisobenzone | 4065-45-6 | – | | – | (290) | 3.5 | – | – | – | – | – | – | – |
| *Phototoxic drugs* | | | | | | | | | | | | | | |
| 3 | Acridine | 260-94-6 | + | + | + | 354 | 2.8 | + | + | + | + | + | + | + |
| 4 | Acridine HCl | 17784-47-3 | + | + | + | 354 | 2.6 | + | + | + | + | + | + | + |
| 5 | Amiodarone HCl | 19774-82-4 | + | + | + | (290) | 5.4 | + | + | I | I | I | I | I |
| 6 | Chlorpromazine HCl | 69-09-0 | + | + | + | 304 | 1.7 | + | + | + | + | + | + | + |
| 7 | Doxycycline HCl | 10592-13-9 | + | + | + | (290) | 3.7 | + | + | + | + | + | + | + |
| 8 | Fenofibrate | 49562-28-9 | + | | + | (290) | 3.5 | + | I | + | + | + | + | I |
| 9 | Furosemide | 54-31-9 | +/– | | + | (290) | 2.7 | + | + | + | + | + | + | + |
| 10 | Ketoprofen | 22071-15-4 | + | – | + | (290) | 2.1 | + | + | + | + | + | + | + |
| 11 | 6-Methylcoumarin | 92-48-8 | + | + | + | (290) | 3.2 | + | + | + | + | + | + | + |
| 12 | 8-Methoxypsoralen | 298-81-7 | + | + | + | 300 | 3.7 | + | + | + | + | + | + | + |
| 13 | Nalidixic acid | 389-08-2 | + | + | + | 331 | 3.2 | + | + | + | + | + | + | + |
| 14 | Nalidixic acid (Na salt) | 3374-05-8 | + | + | + | 333 | 3.0 | + | + | + | + | + | + | + |
| 15 | Norfloxacin | 70458-96-7 | + | + | + | 323 | 3.6 | + | + | + | + | + | + | + |
| 16 | Ofloxacin | 82419-36-1 | + | + | + | (290) | 8.4 | + | + | + | + | + | + | + |
| 17 | Piroxicam | 36322-90-4 | – | – | + | 352 | 3.3 | + | + | + | + | + | + | + |
| 18 | Promethazine HCl | 58-33-3 | + | | + | 297 | 1.6 | + | + | + | + | + | + | + |
| 19 | Rosiglitazone | 122320-73-4 | + | | | 311 | 1.8 | + | + | + | + | + | + | + |
| 20 | Tetracycline | 60-54-8 | + | + | + | (290) | 3.8 | + | + | + | + | + | + | + |
| *Phototoxic chemicals* | | | | | | | | | | | | | | |
| 21 | Anthracene | 120-12-7 | + | + | + | 355 | 2.3 | I | I | + | I | I | I | + |
| 22 | Avobenzone | 70356-09-1 | + | – | + | 354 | 7.7 | + | + | + | + | + | I | + |
| 23 | Bithionol | 97-18-7 | + | + | + | 321 | 2.5 | + | + | + | + | + | + | + |
| 24 | Hexachlorophene | 70-30-4 | – | – | + | 300 | 2.4 | + | + | + | + | + | + | + |
| 25 | Rose bengal | 632-69-9 | + | – | + | 549 | 19.3 | + | + | + | + | + | + | + |
| *Non-phototoxic drugs* | | | | | | | | | | | | | | |
| 26 | Aspirin | 50-78-2 | – | | | (290) | 0.1 | – | – | – | – | – | – | – |
| 27 | Benzocaine | 94-09-7 | – | | | (290) | 4.3 | – | – | – | – | – | – | – |
| 28 | Erythromycin | 114-07-8 | – | | | (290) | 0 | – | – | – | – | – | – | – |
| 29 | Phenytoin | 57-41-0 | – | | | (290) | 0 | + | + | + | + | + | + | + |
| 30 | Penicillin G | 113-98-4 | – | | | (290) | 0 | + | + | + | + | + | + | + |
| *Non-phototoxic chemicals* | | | | | | | | | | | | | | |
| 31 | Bumetrizole | 3896-11-5 | – | | | 306 | 3.9 | I | I | I | I | I | I | I |
| 32 | Camphor sulfonic acid | 3144-16-9 | – | | | (290) | 0 | – | – | – | – | – | – | – |
| 33 | Chlorhexidine | 55-56-1 | – | | – | (290) | 1.3 | – | – | + | – | + | – | + |
| 34 | Cinnamic acid | 140-10-3 | – | | | (290) | 3.4 | – | + | + | – | + | + | – |
| 35 | Drometrizole | 2440-22-4 | – | | | 295 | 3.9 | I | I | I | I | I | I | I |
| 36 | L-Histidine | 71-00-1 | – | | | (290) | 0 | + | + | + | + | + | + | + |
| 37 | Methylbenzylidene camphor | 36861-47-9 | – | – | – | 304 | 9.2 | I | I | I | + | I | I | I |
| 38 | Octrizole | 3147-75-9 | – | | | 296 | 4.0 | I | I | + | I | I | I | + |
| 39 | Octyl methacrylate | 688-84-6 | – | | | (290) | 0 | I | I | + | I | I | I | I |
| 40 | Octyl methoxycinnamate | 5466-77-3 | – | – | – | (290) | 3.0 | I | I | I | + | + | I | I |
| 41 | Octyl salicylate | 118-60-5 | – | – | – | (290) | 1.5 | I | I | I | I | + | I | I |
| 42 | PABA | 150-13-0 | – | – | | (290) | 2.4 | – | – | – | – | – | – | – |
| 43 | SDS | 151-21-3 | – | | | (290) | 0 | – | I | I | + | – | I | I |
| 44 | UV-571 | 125304-04-3 | – | | | (290) | 1.9 | I | I | I | I | I | I | I |

[a] If the peak wavelengths were shorter than the lower limit of UVB (290 nm), the absorbance at 290 nm is shown in parentheses.
[b] +, positive; –, negative; and I, inconclusive.

remaining 42 test chemicals were coded by the VMT and supplied with essential information (physical state, weight or volume of the chemicals, specific density for liquids, storage instructions, molecular weight, and conversion factor). Safety information of the test chemicals was also provided to an appropriate individual within the organization who was not involved in the study, and could be accessed only in case of an emergency. In all cases, the safety information was not accessed by the study directors up to the end of all experiments in the validation study. The identity of the coded chemicals was made known to the study directors at the VMT meeting after all the experiments had been completed and all experimental data had been submitted to the VMT.

### 2.4. ROS assay protocol

#### 2.4.1. Apparatuses

Two types of solar simulator were employed for the previous and present validation studies. In Lab#1–3, the ROS assay was conducted using the Atlas Suntest CPS series (CPS plus in Lab# 1 and 3, and CPS in Lab#2; Atlas Material Technology LLC, Chicago, USA) equipped with a xenon arc lamp (1500 W, Atlas #56-0017-94). In Lab#4–7, Seric SXL-2500V2 was employed for the ROS assay, in which a xenon arc lamp (Seric #SX25001) was installed. A UV filter was installed to adapt the spectrum of the artificial light source to that of natural daylight, and both the Atlas Suntest CPS series and Seric SXL-2500V2 had a high irradiance capability that met CIE85/1989 daylight simulation requirements (Fig. 1).

In Lab#1–3, the irradiation test was carried out at 25 °C with an irradiance of ca. 2.0 mW/cm$^2$ as determined using the calibrated UVA detector Dr. Hönle #0037 (Dr. Hönle, München, Germany) delivered from the VMT. In Lab#4–7, irradiance conditions were optimized to meet the acceptance criteria for a valid assay {quinine (**1**): singlet oxygen ($\Delta A_{440nm} \times 10^3$), ≧150; and superoxide ($\Delta A_{560nm} \times 10^3$), ≧200; and sulisobenzone (**2**): singlet oxygen ($\Delta A_{440nm} \times 10^3$), <25; and superoxide ($\Delta A_{560nm} \times 10^3$), <20}. A quartz reaction container for high-throughput ROS assay (Onoue et al., 2008a) was constructed by Ozawa Science (Aichi, Japan) and supplied from the VMT.

#### 2.4.2. Preparation of test chemicals and controls

Stock solutions of the controls were prepared at 10 mM in DMSO, divided into some tubes, and stored in a freezer for up to 1 month. According to the chromatographic analysis, these stock solutions were stable for at least 1 month under the storage conditions. The stock solution was thawed just before the experiment and used within a day. The coded chemicals were dissolved in DMSO at concentrations of 0.1, 1, and 10 mM just before use under UV-cut illumination or shade. All preparations were kept protected from light.

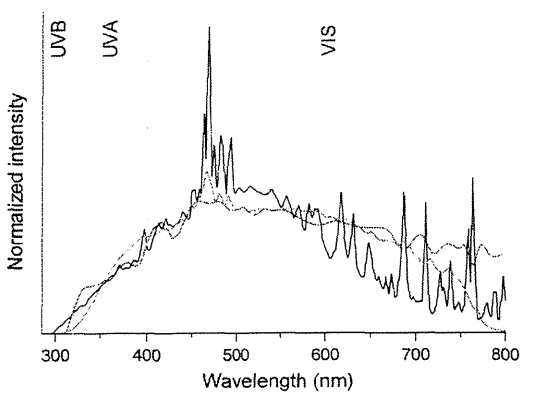


**Fig. 1.** Spectral patterns of simulated sunlight in Atlas Suntest CPS series, Seric SXL-2500V2, and standard daylight (CIE85/1989). Black line, simulated sunlight emitted from Atlas Suntest CPS series; green line, from Seric SXL-2500V2; and red line, standard daylight (CIE85/1989). (For interpretation of the references to color in this figure legend, the reader is referred to the web version of this article.)

#### 2.4.3. ROS assay procedure

The ROS assay was designed to detect both singlet oxygen and superoxide generated from photo-irradiated chemicals (Onoue et al., 2008a; Onoue et al., 2008c). Briefly, singlet oxygen was measured in an aqueous solution by spectrophotometrically monitoring the bleaching of *p*-nitrosodimethylaniline at 440 nm using imidazole as a selective acceptor of singlet oxygen. Samples, containing the tested chemical (20–200 μM), *p*-nitrosodimethylaniline (50 μM), and imidazole (50 μM) in 20 mM sodium phosphate buffer (NaPB, pH 7.4), were mixed in a tube. Two hundreds microliters of the sample was transferred into a well of a plastic 96-well plate (clear, untreated, flat-bottomed) and checked for precipitation under a microscope (×100) before light exposure. The plate was subjected to the measurement of absorbance at 440 nm using a microplate spectrophotometer. The plate was fixed in the quartz reaction container with a quartz cover, and then irradiated with the simulated sunlight for 1 h. After agitation on a plate shaker, the UV absorbance at 440 nm was measured. For the determination of superoxide, samples containing the tested chemical (20–200 μM) and NBT (50 μM) in 20 mM NaPB were irradiated with the simulated sunlight for 1 h, and the reduction in NBT was measured by the increase in absorbance at 560 nm in the same manner as the singlet oxygen determination. Experiments were performed in triplicate wells in three independent runs. As the final concentration, 200 μM test chemical solutions should be subjected to the ROS assay. However, when precipitation could be observed at 200 μM under the optical microscope, additional experiments should be performed under appropriate dilution (20, 50, or 100 μM). When precipitation was observed at 20 μM in the reaction mixture, further experiments were not needed.

#### 2.4.4. Criteria for data acceptance and judgment

The criteria for acceptability of a valid assay were (i) no precipitation of the test chemical in the reaction mixture before light exposure, (ii) no lack of data for positive control, negative control, blank, and the chemical, and (iii) 0.02–1.5 for each net absorbance for the controls and the chemical.

According to the result (mean of triplicate determinations) from the ROS assay, photoreactivity for each test chemical should be judged to be (i) positive with singlet oxygen ($\Delta A_{440nm} \times 10^3$): 25 or more; and/or superoxide ($\Delta A_{560nm} \times 10^3$): 20 or more, or (ii) negative with singlet oxygen: less than 25 ($\Delta A_{440nm} \times 10^3$), and superoxide ($\Delta A_{560nm} \times 10^3$): less than 20. From the mean values of 3 independent experiments, a final decision should be made as follows: (i) positive: above the threshold level for singlet oxygen or superoxide; or (ii) negative: below the threshold level for both singlet oxygen and superoxide.

## 3. Results and discussion

### 3.1. Optimization of irradiance conditions for transferable assay

A previous validation study demonstrated the satisfactory accuracy, precision, and prediction capacity of ROS assay using the Atlas Suntest CPS series at an irradiance intensity of ca. 2.0 mW/m$^2$ (Onoue et al., 2013). According to the results from preliminary studies with a focus on irradiance conditions, ROS assay data on quinine

(**1**), a typical phototoxin (Moore, 2002), and sulisobenzone (**2**), a non-phototoxic chemical (Portes et al., 2002), using the Seric SXL-2500V2 (Lab#4–7) at an intensity of 3.0–5.0 mW/cm$^2$ (Lab#4, 4.0 mW/cm$^2$; Lab#5, 5.0 mW/cm$^2$; Lab#6, 3.5 mW/cm$^2$; Lab#7, 3.0 mW/cm$^2$), were relatively in agreement with those with the Suntest CPS series (Lab#1–3) at ca. 2.0 mW/cm$^2$. As observed in the Atlas Suntest CPS series (Lab#1–3), in the Seric SXL-2500V2 (Lab#4–7), quinine (**1**: 200 μM) had the ability to generate both singlet oxygen and superoxide under UV/VIS exposure (ca. 3.0–5.0 mW/cm$^2$) for 1 h, whereas ROS generation from irradiated sulisobenzone (**2**: 200 μM) was negligible. The optimized irradiance conditions for Seric SXL-2500V2 produced reliable ROS data to meet the acceptance criteria for a valid assay {quinine (**1**): singlet oxygen ($\Delta A_{440nm} \times 10^3$), ≧150; and superoxide ($\Delta A_{560nm} \times 10^3$), ≧200; and sulisobenzone (**2**): singlet oxygen ($\Delta A_{440nm} \times 10^3$), <25; and superoxide ($\Delta A_{560nm} \times 10^3$), <20}. Since the SXL-2500V2 was originally developed for *in vitro* phototoxicity assay, the cytotoxic UVB and UVC region was removed by the UV filter system (Fig. 1). In contrast, the light spectrum from the Suntest CPS series involves partial UVB, and this slight difference in the spectral pattern of emitted light might explain in part the requirement of a higher optimal intensity of simulated sunlight for the SXL-2500V2.

Under the optimized irradiance conditions, a prevalidation study was conducted to assess transferability from lead laboratory to participating laboratories and intra-/inter-laboratory reproducibility using 13 uncoded chemicals. This prevalidation study was undertaken for the training of laboratory personnel, and refinement of the protocol and data analysis sheet. All the participating laboratories produced similar outcomes from the ROS assay on the 13 uncoded chemicals (data not shown). From these observations, even though different solar simulators were used for the ROS assay, satisfactory inter-laboratory reproducibility could be observed among Lab#1–7 as long as the irradiance conditions were optimized.

### 3.2. Intra- and inter-laboratory reproducibility for two standard chemicals

To assess the precision of the ROS assay using SXL-2500V2, repeated ROS assay was carried out for quinine (**1**: 200 μM) and sulisobenzone (**2**: 200 μM) in Lab#4–7 (Fig. 2). The intra-day precision of the ROS assay was evaluated by analyzing 9 samples of quinine (**1**) or sulisobenzone (**2**) solutions at 200 μM. Although no significant generation of ROS was observed for sulisobenzone (**2**), quinine (**1**) was found to be highly photoreactive as evidenced by potent ROS generation {singlet oxygen ($\Delta A_{440nm} \times 10^3$): ca. 390–510; and superoxide ($\Delta A_{560nm} \times 10^3$): ca. 260–280}. The intra-day coefficients of variation (CV) for the detection of singlet oxygen and superoxide generated from irradiated quinine (**1**) were found to range from 3.3% to 6.2%, and 1.7% to 9.4%, respectively. In addition, the inter-day CV values for quinine (**1**) varied from 2.7% to 5.5% for singlet oxygen, and 3.1% to 6.9% for superoxide. These observations were in agreement with the outcomes from the previous validation study using the Atlas Suntest CPS series (Onoue et al., 2013), showing similar ROS data {singlet oxygen ($\Delta A_{440nm} \times 10^3$): ca. 370–530; and superoxide ($\Delta A_{560nm} \times 10^3$): ca. 280–400} and low CV values (<10%) in all the participating laboratories (Lab#1–3). These findings suggested good intra- and inter-day precision, and the ROS assay could be considered reproducible across experiments and across laboratories even though different solar simulators were employed.

In addition to the intra-laboratory precision, the inter-laboratory reproducibility within Lab#4–7 was assessed under the same

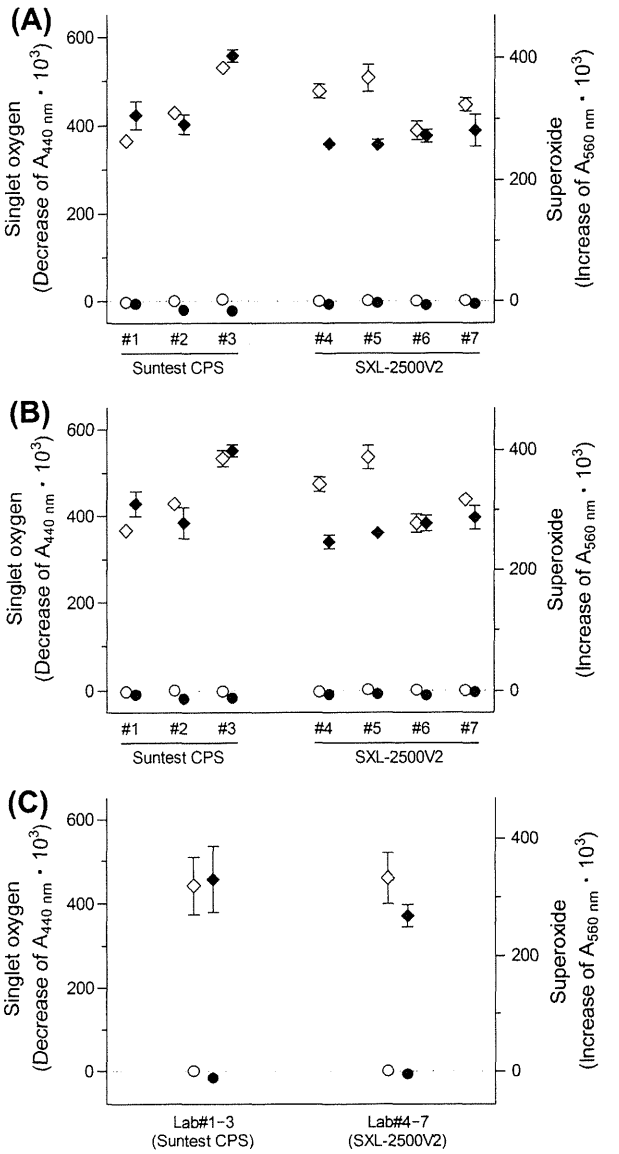


**Fig. 2.** Intra- and inter-laboratory reproducibility on ROS measurement in 2 different solar simulators. (A) Intra-laboratory reproducibility (intra-day), (B) intra-laboratory reproducibility (inter-day), and (C) inter-laboratory reproducibility. The ROS assay on quinine (**1**) and sulisobenzone (**2**) at a concentration of 200 μM was conducted in 7 laboratories employing the Atlas Suntest CPS series (ca. 2.0 mW/cm$^2$, Lab#1–3) or Seric SXL-2500V2 (ca. 3.0–5.0 mW/cm$^2$, Lab#4–7). ◇, singlet oxygen for quinine (**1**); ◆, superoxide; ○, singlet oxygen for sulisobenzone (**2**); and ●, superoxide. Data represent mean ± SD of three repeated experiments for intra-day ($n = 9$) precision and three repeated experiments for inter-day precision (days 1, 2, and 3; $n = 9$).

assay protocol and experimental conditions, except for optimized irradiance. In all the laboratories (Lab#4–7), there appeared to be significant ROS generation from UV-exposed quinine (**1**: 200 μM) with CV values of 13.2% (singlet oxygen) and 7.1% (superoxide). The inter-laboratory reproducibility in the Suntest CPS series (Lab#1–3) was found to be 15.4% for singlet oxygen and 17.0% for superoxide. Intra- and inter-laboratory variability for SXL-2500V2 seemed to be slightly lower than that for the Suntest CPS series. Thus, the satisfactory results for inter-laboratory reproducibility would be indicative of transferability and precision of the

**Table 2**
Outcomes from ROS assay using seric SXL-2500V2 (Lab#4–7).

| No. | Chemical name | | Lab#4 | | | Lab#5 | | | Lab#6 | | | Lab#7 | | |
|---|---|---|---|---|---|---|---|---|---|---|---|---|---|---|
| | | | 1st | 2nd | 3rd | 1st | 2nd | 3rd | 1st | 2nd | 3rd | 1st | 2nd | 3rd |
| ***Phototoxic drugs*** | | | | | | | | | | | | | | |
| 3 | Acridine | $^1O_2$ | 287 | 300 | 309 | 325 | 307 | 311 | 238 | 247 | 241 | 236 | 268 | 272 |
| | | $O_2^-$ | 142 | 148 | 150 | 157 | 112 | 162 | 203 | 208 | 216 | 169 | 178 | 180 |
| 4 | Acridine HCl | $^1O_2$ | 286 | 308 | 297 | 317 | 317 | 317 | 263 | 245 | 240 | 264 | 263 | 256 |
| | | $O_2^-$ | 142 | 143 | 144 | 108 | 116 | 138 | 191 | 261 | 184 | 157 | 157 | 160 |
| 5 | Amiodarone HCl | $^1O_2$ | – | – | – | – | – | – | – | – | – | – | – | – |
| | | $O_2^-$ | – | – | – | – | – | – | – | – | – | 5 | -7 | -6 |
| 6 | Chlorpromazine HCl | $^1O_2$ | 29 | 29 | 46 | 52 | 72 | 68 | -8 | 7 | -9 | 13 | 14 | 6 |
| | | $O_2^-$ | 86 | 77 | 73 | 91 | 82 | 92 | 79 | 75 | 80 | 77 | 80 | 77 |
| 7 | Doxycycline HCl | $^1O_2$ | 310 | 299 | 289 | 430 | 426 | 429 | 206 | 218 | 261 | 279 | 305 | 291 |
| | | $O_2^-$ | 318 | 299 | 299 | 377 | 375 | 384 | 324 | 319 | 365 | 341 | 372 | 351 |
| 8 | Fenofibrate | $^1O_2$ | *125* | *125* | *140* | *209* | *214* | *215* | *93* | *99* | *119* | – | – | – |
| | | $O_2^-$ | *-4* | *-4* | *-8* | *-2* | *-11* | *-7* | *-11* | *-13* | *-14* | *5* | *-1* | *0* |
| 9 | Furosemide | $^1O_2$ | 108 | 108 | 118 | 114 | 117 | 127 | 79 | 77 | 71 | 85 | 80 | 75 |
| | | $O_2^-$ | 23 | 21 | 31 | 34 | 33 | 36 | 35 | 35 | 32 | 34 | 33 | 25 |
| 10 | Ketoprofen | $^1O_2$ | 219 | 223 | 204 | 220 | 210 | 199 | 196 | 189 | 205 | 207 | 175 | 173 |
| | | $O_2^-$ | 110 | 107 | 98 | 140 | 136 | 133 | 117 | 135 | 144 | 109 | 103 | 92 |
| 11 | 6-Methylcoumarin | $^1O_2$ | 176 | 161 | 127 | 174 | 141 | 150 | 90 | 88 | 93 | 136 | 109 | 126 |
| | | $O_2^-$ | 89 | 79 | 54 | 108 | 109 | 97 | 102 | 99 | 107 | 61 | 37 | 64 |
| 12 | 8-Methoxypsoralen | $^1O_2$ | 108 | 118 | 108 | 147 | 111 | 123 | 50 | 47 | 59 | 62 | 62 | 72 |
| | | $O_2^-$ | 47 | 53 | 40 | 51 | 51 | 72 | 75 | 82 | 79 | 34 | 23 | 32 |
| 13 | Nalidixic acid | $^1O_2$ | 143 | 141 | 151 | 147 | 146 | 148 | 133 | 119 | 112 | 129 | 128 | 125 |
| | | $O_2^-$ | 195 | 212 | 215 | 185 | 226 | 108 | 479 | 457 | 476 | 252 | 242 | 236 |
| 14 | Nalidixic acid (Na salt) | $^1O_2$ | 163 | 143 | 143 | 140 | 138 | 156 | 113 | 110 | 111 | 124 | 118 | 126 |
| | | $O_2^-$ | 187 | 206 | 204 | 146 | 194 | 263 | 316 | 471 | 435 | 246 | 253 | 256 |
| 15 | Norfloxacin | $^1O_2$ | 231 | 225 | 203 | 257 | 242 | 258 | 140 | 139 | 142 | 214 | 200 | 217 |
| | | $O_2^-$ | 70 | 72 | 75 | 102 | 83 | 95 | 109 | 110 | 111 | 76 | 92 | 87 |
| 16 | Ofloxacin | $^1O_2$ | 173 | 184 | 177 | 200 | 193 | 198 | 153 | 143 | 141 | 127 | 124 | 133 |
| | | $O_2^-$ | 320 | 295 | 291 | 269 | 326 | 287 | 469 | 458 | 482 | 287 | 394 | 400 |
| 17 | Piroxicam | $^1O_2$ | 347 | 306 | 302 | 432 | 407 | 411 | 233 | 258 | 211 | 247 | 246 | 258 |
| | | $O_2^-$ | *113* | *105* | *98* | *139* | *162* | *128* | *246* | *249* | *247* | *70* | *62* | *71* |
| 18 | Promethazine HCl | $^1O_2$ | 121 | 128 | 127 | 149 | 151 | 147 | 50 | 53 | 62 | 114 | 124 | 117 |
| | | $O_2^-$ | 28 | 24 | 22 | 28 | 29 | 18 | 18 | 17 | 19 | 28 | 27 | 27 |
| 19 | Rosiglitazone | $^1O_2$ | 65 | 63 | 71 | 49 | 51 | 48 | 33 | 26 | 42 | 38 | 34 | 46 |
| | | $O_2^-$ | *33* | *32* | *33* | *78* | *79* | *71* | *73* | *92* | *56* | *53* | *66* | *65* |
| 20 | Tetracycline | $^1O_2$ | 208 | 257 | 226 | 346 | 333 | 328 | 153 | 146 | 150 | 224 | 234 | 231 |
| | | $O_2^-$ | 160 | 159 | 151 | 220 | 246 | 235 | 196 | 195 | 183 | 211 | 223 | 255 |
| ***Phototoxic chemicals*** | | | | | | | | | | | | | | |
| 21 | Anthracene | $^1O_2$ | – | – | – | – | – | – | – | – | – | – | – | – |
| | | $O_2^-$ | – | – | – | – | – | – | – | – | – | *69* | *86* | *36* |
| 22 | Avobenzone | $^1O_2$ | *191* | *228* | *238* | *89* | *91* | *80* | – | – | – | – | – | – |
| | | $O_2^-$ | *1* | *15* | *-12* | *80* | *50* | *54* | – | – | – | *31* | *34* | *40* |
| 23 | Bithionol | $^1O_2$ | 129 | 151 | 140 | 166 | 110 | 167 | 70 | 70 | 81 | 128 | 148 | 155 |
| | | $O_2^-$ | – | – | – | 21 | 18 | 22 | 18 | 23 | 15 | – | – | – |
| 24 | Hexachlorophene | $^1O_2$ | 106 | 99 | 140 | 150 | 149 | 142 | 120 | 94 | 101 | 134 | 133 | 141 |
| | | $O_2^-$ | 0 | 0 | 0 | -2 | -9 | -3 | -5 | -5 | -2 | – | – | – |
| 25 | Rose Bengal | $^1O_2$ | 660 | 704 | 708 | 818 | 836 | 816 | 693 | 659 | 645 | 630 | 661 | 670 |
| | | $O_2^-$ | NA | NA | NA | NA | NA | NA | NA | NA | NA | NA | NA | NA |
| ***Non-phototoxic drugs*** | | | | | | | | | | | | | | |
| 26 | Aspirin | $^1O_2$ | 1 | 0 | 0 | -1 | 1 | -2 | 4 | 2 | 3 | -1 | -2 | 1 |
| | | $O_2^-$ | -2 | -1 | -2 | -3 | -8 | -2 | 0 | 0 | -1 | -1 | 0 | -1 |
| 27 | Benzocaine | $^1O_2$ | 1 | 1 | 1 | 1 | -2 | -1 | 0 | 0 | 7 | -1 | 0 | 5 |
| | | $O_2^-$ | 7 | 4 | 5 | 9 | 7 | 10 | 5 | 6 | 4 | 1 | -7 | 1 |
| 28 | Erythromycin | $^1O_2$ | -2 | -10 | -1 | -7 | -4 | 2 | -3 | -2 | -3 | 3 | -10 | -7 |
| | | $O_2^-$ | 9 | 2 | 1 | 3 | 2 | 4 | 5 | 4 | 6 | -1 | 3 | 1 |
| 29 | Phenytoin | $^1O_2$ | 0 | 2 | 0 | 0 | 6 | -1 | -3 | -2 | -2 | 0 | -7 | 1 |

| | | | | | | | | | | | | | | |
|---|---|---|---|---|---|---|---|---|---|---|---|---|---|---|
| | $O_2^{\cdot-}$ | 63 | 62 | 70 | 93 | 82 | 101 | 75 | 65 | 57 | 53 | 37 | 12 |
| | $^1O_2$ | -1 | 2 | 1 | 1 | 8 | 0 | 0 | 3 | 2 | 1 | 2 | -1 |
| **30** Penicillin G | $O_2^{\cdot-}$ | 39 | 39 | 33 | 49 | 43 | 47 | 37 | 37 | 44 | 13 | 9 | 5 |
| ***Non-phototoxic chemicals*** | | | | | | | | | | | | | | |
| | $^1O_2$ | *-10* | *-18* | *-36* | *-13* | *-18* | *-8* | *-4* | *-1* | *1* | – | – | – |
| **31** Bumetrizole | $O_2^{\cdot-}$ | *8* | *7* | *13* | – | – | – | *16* | *13* | *18* | *6* | *8* | *10* |
| | $^1O_2$ | 0 | 0 | -1 | 0 | 1 | -2 | 5 | 0 | -1 | 3 | 1 | 0 |
| **32** Camphor sulfonic acid | $O_2^{\cdot-}$ | -2 | 0 | -1 | -1 | -6 | -2 | -2 | -3 | 0 | -1 | -1 | 4 |
| | $^1O_2$ | 5 | 4 | 7 | -1 | 2 | 4 | 8 | -6 | 18 | 4 | 1 | -1 |
| **33** Chlorhexidine | $O_2^{\cdot-}$ | 13 | 20 | 16 | 20 | 28 | 27 | 16 | 17 | 14 | 25 | 24 | 28 |
| | $^1O_2$ | 0 | 0 | 0 | -1 | 9 | 0 | 0 | 2 | -1 | 2 | 0 | 1 |
| **34** Cinnamic acid | $O_2^{\cdot-}$ | 10 | 13 | 7 | 33 | 45 | 40 | 43 | 36 | 32 | 10 | 3 | 2 |
| | $^1O_2$ | – | – | – | – | – | – | *5* | *1* | *3* | – | – | – |
| **35** Drometrizole | $O_2^{\cdot-}$ | – | – | – | – | – | – | *3* | *6* | *2* | – | – | – |
| | $^1O_2$ | -1 | 1 | 0 | -2 | -2 | -1 | 1 | 0 | -1 | -1 | -4 | 1 |
| **36** L-histidine | $O_2^{\cdot-}$ | 78 | 74 | 57 | 112 | 101 | 110 | 42 | 31 | 28 | 91 | 85 | 85 |
| | $^1O_2$ | *36* | *25* | *44* | *30* | *11* | *25* | *-1* | *-3* | *-1* | *-2* | *1* | *0* |
| **37** Methylbenzylidene camphor | $O_2^{\cdot-}$ | *-17* | *-24* | *-26* | *-10* | *-12* | *-20* | *2* | *3* | *1* | *-5* | *-2* | *0* |
| | $^1O_2$ | *-6* | *-11* | *-18* | *-14* | *-24* | *-28* | – | – | – | *-21* | *-23* | *-34* |
| **38** Octrizole | $O_2^{\cdot-}$ | – | – | – | – | – | – | – | – | – | *28* | *27* | *25* |
| | $^1O_2$ | *4* | *0* | *3* | *18* | *25* | *18* | *4* | *7* | *4* | – | – | – |
| **39** Octyl methacrylate | $O_2^{\cdot-}$ | *-1* | *-2* | *-2* | *7* | *4* | *3* | *-3* | *-3* | *-1* | *-15* | *3* | *-1* |
| | $^1O_2$ | *12* | *10* | *11* | *2* | *11* | *7* | *20* | *14* | *17* | – | – | – |
| **40** Octyl methoxycinnamate | $O_2^{\cdot-}$ | *23* | *26* | *16* | *35* | *21* | *17* | *10* | *17* | *17* | *-2* | *-4* | *0* |
| | $^1O_2$ | *4* | *6* | *4* | *7* | *18* | *5* | *1* | *4* | *3* | *7* | *3* | *4* |
| **41** Octyl salicylate | $O_2^{\cdot-}$ | *16* | *12* | *14* | *42* | *30* | *33* | *17* | *14* | *11* | *3* | *-1* | *-2* |
| | $^1O_2$ | -1 | 1 | -1 | 0 | 9 | 1 | 0 | 2 | 1 | 3 | -1 | 1 |
| **42** PABA | $O_2^{\cdot-}$ | 0 | 0 | 0 | -3 | -5 | -5 | -6 | -8 | -5 | -7 | 0 | -3 |
| | $^1O_2$ | 5 | 10 | 9 | 5 | 15 | 8 | 7 | 9 | 6 | 3 | 1 | -3 |
| **43** SDS | $O_2^{\cdot-}$ | 31 | 22 | 25 | 13 | 19 | 18 | *8* | *10* | *7* | – | – | – |
| | $^1O_2$ | *12* | *3* | *5* | *-10* | *-3* | *-3* | – | – | – | – | – | – |
| **44** UV-571 | $O_2^{\cdot-}$ | *15* | *18* | *23* | – | – | – | – | – | – | *12* | *17* | *13* |

$^1O_2$, singlet oxygen (decrease in $A_{440nm} \times 10^3$), and $O_2^{\cdot-}$, superoxide (increase in $A_{560nm} \times 10^3$). ROS assay was basically carried out for test chemicals at a concentration of 200 μM, and ROS data on the diluted chemicals are boxed (100 μM) or emphasized with black (20 μM) and gray (50 μM). Each value represents the mean of three determinations.

ROS assay employing different solar simulators with optimized irradiance conditions.

### 3.3. Assay performance

#### 3.3.1. Unevaluable chemicals

In accordance with the standardized protocol, the ROS assay was carried out for 42 coded chemicals, consisting of 23 known phototoxins (**3–25**) and 19 non-phototoxic drugs/chemicals (**26–44**) in Lab#4–7, to verify its predictive capacity (Table 2). Because of the limited solubility in assay buffer, 26–28 chemicals (62–67% of the total) were precipitated in assay buffer before and/or after irradiation, and thus are unevaluable at a concentration of 200 μM. Therefore, the ROS assay on these unevaluables was carried out under appropriate dilution (final concentration, 20, 50, or 100 μM), although ROS assay on amiodarone HCl (**5**), anthracene (**21**), and drometrizole (**35**) was still challenging in most participating laboratories. In addition to the solubility issues, spectral interference on ROS determination was seen in rose bengal (**25**). Assay solution of rose bengal (**25**) exhibited intense UV/VIS absorption with a molar extinction coefficient of 19,300 $M^{-1}$ $cm^{-1}$ at 549 nm in methanol (Table 1), leading to severe spectral interference at the defined wavelength number for the determination of superoxide (560 nm). Herein, only singlet oxygen was measured for rose bengal (**25**). To clarify possible interference in ROS determination, UV/VIS absorption of other coded chemicals was also determined in 20 mM NaPB or methanol (Table 1). In the current chemical set, no significant absorption was seen in the VIS region, so spectral interference on ROS determination would be negligible

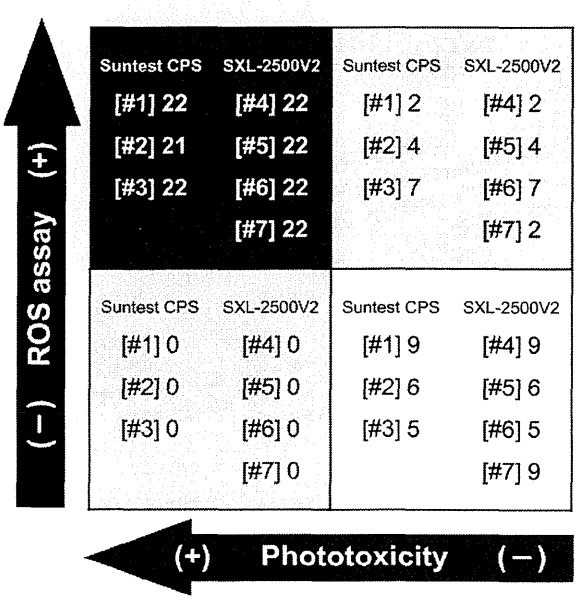


**Fig. 3.** Positive and negative predictivity of the ROS assay in Lab#1–7.

**Table 3**
Applicability and predictive capacity of ROS assay in 7 participating laboratories.

| | Suntest CPS series (Atlas) | | | SXL-2500V2 (Seric) | | | |
|---|---|---|---|---|---|---|---|
| | Lab#1 | Lab#2 | Lab#3 | Lab#4 | Lab#5 | Lab#6 | Lab#7 |
| Evaluable chemicals (%) | 78.6 | 73.8 | 81.0 | 81.0 | 81.0 | 71.4 | 76.2 |
| Sensitivity (%) | 100.0 | 100.0 | 100.0 | 100.0 | 100.0 | 100.0 | 100.0 |
| Specificity (%) | 81.8 | 60.0 | 41.7 | 53.8 | 46.2 | 60.0 | 63.6 |
| Positive predictivity (%) | 91.7 | 84.0 | 75.9 | 77.8 | 75.0 | 83.3 | 84.0 |
| Negative predictivity (%) | 100.0 | 100.0 | 100.0 | 100.0 | 100.0 | 100.0 | 100.0 |

for other chemicals. Some drugs with potent chromophores and cosmetic chemicals, especially dyes and sunscreens, sometimes have intense VIS absorption, so careful consideration should be made on this issue for reliable photosafety assessment. These drawbacks were already pointed out in the previous validation study (Onoue et al., 2013), and the photosafety of these unevaluables might be assessed by other photosafety testing methods and/or a new ROS assay protocol using appropriate solubilizers (Onoue et al., 2014; Seto et al., 2013).

*3.3.2. Predictive capacity*

A previous investigation demonstrated that the photoreactivity of compounds tested at 200 μM could be predicted according to the discrimination criteria of ROS data {25 ($\Delta A_{440nm} \times 10^3$) for singlet oxygen and 20 ($\Delta A_{560nm} \times 10^3$) for superoxide} (Onoue et al., 2008a). These criteria would still be available for positive prediction of the diluted samples in the ROS assay; however, negative predictions would be challenging under dilution since ROS generation from some phototoxins at a low concentration was found to be very weak or negligible (Onoue et al., 2013). Herein, negative prediction for the diluted samples should be made carefully, and the diluted samples with a subthreshold level should be identified to be unevaluable in the ROS assay. In accordance with these criteria, the photoreactivity and photosafety on 42 coded chemicals were evaluated (Table 2 and Fig. 3). In the 4 participating laboratories (Lab#4–7), 22 phototoxins (20–200 μM) tended to generate ROS under exposure to the simulated sunlight as long as they were soluble in the assay buffer. In contrast, there appeared to be weak photoreactivity for most non-phototoxic drugs/chemicals, although some exhibited potent photoreactivity in a few laboratories. Using the proposed criteria, most phototoxins tested here were correctly identified to be phototoxic in Lab#4–7, whereas some phototoxins were unevaluable due to the poor solubility. Of all 19 non-phototoxic samples, 9–14 compounds (ca. 47–74% of the total negatives) were in the subthreshold region, and, in the participating laboratories, at least 5–9 compounds were found to be non-phototoxic on the basis of ROS data at 200 μM. The negativity for other chemicals could not be fully proven as they were assessed under dilution. Inconsistent predictions were made on weak ROS generators such as chlorhexidine (**33**) and cinnamic acid (**34**), and these would be attributable to the lowered classification criteria. Although lower setting of threshold values might prevent false negative prediction, the slight variation in the ROS assay might lead to discrepant phototoxicity prediction for weak ROS generators. Overall, reproducible prediction could be achieved among participating laboratories (Lab#4–7), in which consistency levels for evaluable phototoxins and non-phototoxic chemicals were found to be 100% and 75%, respectively. The prediction capacity of the ROS assay using two different solar simulators is summarized in Table 3. In both validation studies, ca. 70–80% of coded chemicals were evaluable in the ROS assay at a dilution of 200 μM or under. In the present study (Lab#4–7), the individual specificity was calculated to be ca. 46–64%, and the positive and negative predictivities were found to be ca. 75–84% and 100%. These findings were in agreement with the outcomes from the previous validation study, and the present validation study provided further evidence that the defined classification criteria gave no false negatives compared to the *in vitro/in vivo* phototoxicity.

From these findings, taken together with previous data, the ROS assay would be valuable as first screening to identify the phototoxic potential of drug candidates, and the Seric SXL-200V2 would be applicable to the ROS assay. Use of other solar simulators might also be available for the ROS assay; however, the implementation of a UVB filter in the solar simulator might have a significant impact on ROS data for UVB absorbers, possibly leading to false negative predictions as observed in the 3T3 NRU PT. Thus, in order to ensure the availability and compatibility of other light sources, comprehensive optimization and verification would be necessary before such alternative use.

## 4. Conclusion

In the present validation study, the photochemical reactivities of 42 coded chemicals and 2 standard controls were assessed by the ROS assay using Seric SXL-2500V2, and the outcomes were compared with the previous validation data using the Atlas Suntest CPS series. The ROS assay using two different solar simulators achieved satisfactory transferability of the method, fine intra-/inter-laboratory reproducibility, and predictive capacity. On the basis of the present findings, upon spectral characterization of emitted light and optimization of irradiance conditions, other solar simulators might also be available for ROS assay for photosafety assessment.

## Conflict of interest

None of the authors have any conflicts of interest associated with this study.

## Acknowledgements

This work was supported in part by a Health Labour Sciences Research Grant from The Ministry of Health, Labour and Welfare, Japan. The authors are grateful to Dr. Manfred Liebsch (ZEBET), ICCVAM, ECVAM, and KoCVAM for valuable suggestions throughout this work.

## Appendix A. Supplementary material

Transparency Documents associated with this article can be found, in the online version, at http://dx.doi.org/10.1016/j.tiv.2013.11.014.

## References


Brendler-Schwaab, S., Czich, A., Epe, B., Gocke, E., Kaina, B., Muller, L., Pollet, D., Utesch, D., 2004. Photochemical genotoxicity: principles and test methods. *Report of a CUM task force. Mutat. Res.* 566, 65–91.

Durbize, E., Vigan, M., Puzenat, E., Girardin, P., Adessi, B., Desprez, P.H., Humbert, P.H., Laurent, R., Aubin, F., 2003. Spectrum of cross-photosensitization in 18 consecutive patients with contact photoallergy to ketoprofen: associated photoallergies to non-benzophenone-containing molecules. Contact Dermatitis 48, 144–149.

**The European Agency for the Evaluation of Medicinal Products, Evaluation of Medicines for Human Use, Committee for Proprietary Medicinal Products (EMEA/CPMP), 2002. Note for Guidance on Photosafety Testing, CPMP/SWP/398/01.**

Epstein, J.H., 1983. Phototoxicity and photoallergy in man. J. Am. Acad. Dermatol. 8, 141–147.

Epstein, J.H., Wintroub, B.U., 1985. Photosensitivity due to drugs. Drugs 30, 42–57.

**FDA/CDER, 2002. Guidance for Industry, Photosafety Testing. The Food and Drug Administration, Center for Drug Evaluation and Research.**

**International Conference on Harmonization of Technical Requirements for Registration of Pharmaceuticals for Human Use (ICH), 2013. *ICH* Guideline S10 Guidance on Photosafety Evaluation of Pharmaceuticals (draft).**

Moore, D.E., 1998. Mechanisms of photosensitization by phototoxic drugs. Mutat. Res. 422, 165–173.

Moore, D.E., 2002. Drug-induced cutaneous photosensitivity: incidence, mechanism, prevention and management. Drug Saf. 25, 345–372.

Motley, R.J., Reynolds, A.J., 1989. *Photocontact dermatitis due to isopropyl* and butyl methoxy dibenzoylmethanes (Eusolex 8020 and Parsol 1789). Contact Dermatitis 21, 109–110.

**The Organisation for Economic Co-operation and Development (OECD), 2004. OECD Guideline for Testing of Chemicals, 432, *In vitro* 3T3 NRU Phototoxicity Test.**

Onoue, S., Tsuda, Y., 2006. *Analytical studies on the prediction of photosensitive/* phototoxic potential of pharmaceutical substances. Pharm. Res. 23, 156–164.

Onoue, S., Igarashi, N., Yamada, S., Tsuda, Y., 2008a. High-throughput reactive oxygen species (ROS) assay: An enabling technology for screening the phototoxic potential of pharmaceutical substances. J. Pharm. Biomed. Anal. 46, 187–193.

Onoue, S., Kawamura, K., Igarashi, N., Zhou, Y., Fujikawa, M., Yamada, H., Tsuda, Y., Seto, Y., Yamada, S., 2008b. Reactive oxygen species assay-based risk assessment of drug-induced phototoxicity: classification criteria and application to drug candidates. J. Pharm. Biomed. Anal. 47, 967–972.

Onoue, S., Yamauchi, Y., Kojima, T., Igarashi, N., Tsuda, Y., 2008c. Analytical studies on photochemical behavior of phototoxic substances: effect of detergent additives on singlet oxygen generation. Pharm. Res. 25, 861–868.

Onoue, S., Ochi, M., Gandy, G., Seto, Y., Igarashi, N., Yamauchi, Y., Yamada, S., 2010. High-throughput screening system for identifying phototoxic potential of drug candidates based on derivatives of reactive oxygen metabolites. Pharm. Res. 27, 1610–1619.

Onoue, S., Hosoi, K., Wakuri, S., Iwase, Y., Yamamoto, T., Matsuoka, N., Nakamura, K., Toda, T., Takagi, H., Osaki, N., Matsumoto, Y., Kawakami, S., Seto, Y., Kato, M., Yamada, S., Ohno, Y., Kojima, H., 2013. Establishment and intra-/inter-laboratory validation of a standard protocol of reactive oxygen species assay for chemical photosafety evaluation. J. Appl. Toxicol. 33, 1241–1250.

Onoue, S., Kato, M., Yamada, S., 2014. Development of albuminous reactive oxygen species assay for photosafety evaluation under experimental biomimetic conditions. J. Appl. Toxicol. 34, 158–165.

Peters, B., Holzhutter, H.G., 2002. *In vitro* phototoxicity testing: development and validation of a new concentration response analysis software and biostatistical analyses related to the use of various prediction models. ATLA 30, 415–432.

Portes, P., Pygmalion, M.J., Popovic, E., Cottin, M., Mariani, M., 2002. Use of human reconstituted epidermis Episkin for assessment of weak phototoxic potential of chemical compounds. Photodermatol. Photoimmunol. Photomed. 18, 96–102.

Seto, Y., Hosoi, K., Takagi, H., Nakamura, K., Kojima, H., Yamada, S., Onoue, S., 2012. Exploratory and regulatory assessments on photosafety of new drug entities. Curr. Drug Saf. 7, 140–148.

Seto, Y., Kato, M., Yamada, S., Onoue, S., 2013. Development of micellar reactive oxygen species assay for photosafety evaluation of poorly water-soluble chemicals. Toxicol. *In Vitro* 27, 1838–1846.

Spielmann, H., 1994. *In vitro* phototoxicity testing. The report and recommendations of ECVAM Workshop 2. ATLA 22, 314–348.

Spielmann, H., Balls, M., Brand, M., Doring, B., Holzhutter, H.G., Kalweit, S., Klecak, G., Eplattenier, H.L., Liebsch, M., Lovell, W.W., Maurer, T., Moldenhauer, F., Moore, L., Pape, W.J., Pfannenbecker, U., Potthast, J., De Silva, O., Steiling, W., Willshaw, A., 1994a. EEC/COLIPA project on *in vitro* phototoxicity testing: first results obtained with a Balb/c 3T3 cell phototoxicity assay. Toxicol. *In Vitro* 8, 793–796.

Spielmann, H., Liebsch, M., Doring, B., Moldenhauer, F., 1994b. *First results of an EC/* COLIPA validation project of *in vitro* phototoxicity testing methods. Altex 11, 22–31.

Spielmann, H., Liebsch, M., Pape, W.J., Balls, M., Dupuis, J., Klecak, G., Lovell, W.W., Maurer, T., De Silva, O., Steiling, W., 1995. *EEC/COLIPA in vitro* photoirritancy program: results of the first stage of validation. Curr. Probl. Dermatol. 23, 256–264.

Spielmann, H., Balls, M., Dupuis, J., 1998a. The international EU/COLIPA *in vitro* phototoxicity validation study: results of phase II (blind trial). Part 1: the 3T3 NRU phototoxicity test. Toxicol. *In Vitro* 12, 305–327.

Spielmann, H., Balls, M., Dupuis, J., Pape, W.J., Silva, O., Holzhutter, H.G., Gerberick, F., Liebsch, M., Lovell, W.W., Pfannenbecker, U., 1998b. A study on UV filter chemicals from Annex VII of European Union Directive 76/768/EEC, in the *in vitro* 3T3 NRU phototoxicity test. ATLA 26, 679–708.

Trevisi, P., Vincenzi, C., Chieregato, C., Guerra, L., Tosti, A., 1994. Sunscreen sensitization: a three-year study. Dermatology 189, 55–57.

TOXICOLOGICAL SCIENCES 137(2), 469–477 2014
doi:10.1093/toxsci/kft260
Advance Access publication November 16, 2013

# Photosafety Screening of Phenothiazine Derivatives With Combined Use of Photochemical and Cassette-Dosing Pharmacokinetic Data

Satomi Onoue,[1] Masashi Kato, Ryo Inoue, Yoshiki Seto, and Shizuo Yamada

*Department of Pharmacokinetics and Pharmacodynamics, School of Pharmaceutical Sciences, University of Shizuoka, Shizuoka 422–8526, Japan*

[1]To whom correspondence should be addressed at Department of Pharmacokinetics and Pharmacodynamics, School of Pharmaceutical Sciences, University of Shizuoka, 52-1 Yada, Suruga-ku, Shizuoka 422–8526, Japan. Fax: +81-54-264-5635. E-mail: onoue@u-shizuoka-ken.ac.jp.

Received September 11, 2013; accepted November 5, 2013

**This study aimed to establish an efficient photosafety screening system, employing *in vitro* photochemical and cassette-dosing pharmacokinetic (PK) studies. Eight phenothiazine (PTZ) derivatives were selected as model chemicals, and photochemical characterization and cassette-dosing PK study were carried out. *In vivo* photosafety testing on oral PTZs (100 mg/kg) was also assessed in rats. All the tested PTZs exhibited potent UVA/B absorption with molar extinction coefficients of ca. 3400–4400 $M^{-1}cm^{-1}$. Under exposure to simulated sunlight (2.0 $mW/cm^2$), all PTZs, especially fluphenazine 2HCl (FP) and trifluoperazine 2HCl (TF), tended to generate reactive oxygen species (ROS). Casset-dosing PK studies demonstrated high dermal deposition of FP and TF in rats, and from these findings, taken together with the potent photochemical reactivity, both FP and TF were deduced to be highly phototoxic. In contrast, the phototoxic potential of chlorpromazine HCl (CP) seemed to be low because of moderate ROS generation and limited dermal distribution. Predicted phototoxic risk for PTZs from photochemical and PK data appeared basically to agree with the observed phototoxicity in rats; however, oral CP (100 mg/kg) caused severe phototoxic responses in rats. Metabolites of CP have been recognized to be phototoxic, which might explain in part this false prediction. These findings might also suggest the necessity of complementary testing on drug metabolites for more reliable photosafety evaluation. The combined use of photochemical and PK data might be efficacious for simple and fast prediction of the phototoxic potential of new drug candidates.**

*Key Words:* **phenothiazines; photoreactivity; photosafety assessment; phototoxicity; reactive oxygen species.**

Recently, the level of interest in drug-induced phototoxicity has markedly increased owing to the increased level of ultraviolet (UV) radiation from the sun reaching the earth (Onoue *et al.*, 2009). Phototoxic reactions in skin and eyes can be caused by several classes of injected, orally, or topically applied pharmaceutics at clinical doses (Moore, 1998, 2002). Most phototoxic skin responses result from the systemic administration of the agent, and perceptible adverse effects would lead to a reduction in medication compliance. In addition to the clinical aspects, phototoxicity issues have also thwarted pharmaceutical development; therefore, the pharmaceutical industry, academia, and regulatory agencies have made considerable efforts in the prediction and/or avoidance of phototoxic liability. A number of effective methodologies for evaluating the phototoxic risk of chemicals have been developed over the past few years, and guidance on the photosafety testing of medicinal products was established by regulatory agencies in the United States and European Union in the early 2000s (Seto *et al.*, 2012). These guidelines have described photosafety assessments of tested compounds on the basis of light absorption properties, administration routes, and distribution behaviors in pharmaceutical research and development (EMEA/CPMP, 2002; FDA/CDER, 2002; OECD, 2004). Recently, the issuance of the Step 2 draft ICH S10 photosafety guidance document provided a detailed framework and guidance for photosafety evaluation (ICH, 2013). This draft guideline describes photosafety assessment strategies on the basis of photochemical (UV/VIS measurement and reactive oxygen species [ROS] assay) and photobiochemical properties (3T3 neutral red uptake phototoxicity test), and *in vivo* pharmacokinetic behavior (distribution and retention in the UV-exposed tissues). Strategic screening for photosafety is necessary at the early phase of the drug discovery process and even before introducing drugs into clinical therapy.

A number of analytical and biochemical methodologies for photosafety testing have been developed, including *in silico* prediction models, photochemical screening systems, and *in vitro* phototoxic prediction tools. These *in vitro* photosafety assessments might also be effective for clarifying the mechanism of phototoxicity for tested chemicals in detail; however, the results from *in vitro* photosafety evaluations would not always reflect clinical observations of drug-induced phototoxicity. Herein, further characterization of pharmacokinetics with a focus on skin distribution might ensure prediction of the *in vivo* photosafety of tested chemicals because phototoxic reactions mainly occur in the skin after topical and/or systemic

administration. Previous study also demonstrated that the combined use of *in vitro* photobiochemical/phototoxic and pharmacokinetic data might enable evaluation of *in vivo* phototoxic risk with high clinical relevance (Seto *et al.*, 2011), although several *in vitro* evaluations had to be employed, affecting assay throughput. Recently, photochemical data on pharmaceutics from UV measurement (Henry *et al.*, 2009) and ROS assay (Onoue and Tsuda, 2006; Onoue *et al.*, 2008a) were found to be partly indicative of their photobiochemical and phototoxic properties. In this context, as well as pharmacokinetics, strategic combination use of photochemical data as an alternative to complicated *in vitro* photobiochemical/phototoxic data might lead to simplified photosafety evaluation; however, far less is known about its feasibility.

The major purpose of this study was to develop a new photosafety screening system employing mechanistic photochemical and pharmacokinetic data. Eight phenothiazines (PTZs) were selected as model chemicals because PTZs have been recognized as phototoxins in clinical use (Chignell *et al.*, 1985; Miolo *et al.*, 2006). Photochemical properties of PTZs were assessed by UV spectral analysis and ROS assay according to the validated protocol (Onoue *et al.*, 2013). In this study, to reduce animal usage, a cassette-dosing approach was applied for pharmacokinetic study on PTZs in rats. Systemic exposure of PTZs and the distribution to the UV-exposed tissues after oral cassette dosing in rats were conducted using ultra-performance liquid chromatography equipped with electrospray ionization mass spectrometry (UPLC/ESI-MS), and photosafety evaluation was made on the basis of these photochemical and pharmacokinetic data. An *in vivo* phototoxicity test was also conducted in rats after oral administration of each PTZ to compare the predicted phototoxicity with the observed phototoxic skin responses.

## MATERIALS AND METHODS

***Chemicals.*** According to previous *in vitro*/*in vivo* photosafety information and clinical observations (Corbett *et al.*, 1978; Eberlein-König *et al.*, 1997; Ljunggren and Möller, 1977; Miolo *et al.*, 2006; Viola and Dall'Acqua, 2006), 8 PTZs were selected as model chemicals for this study (Fig. 1). On the basis of previously reported photosafety data (Moore, 2002; Onoue *et al.*, 2013), quinine HCl (QN) and erythromycin (EM) were selected as positive and negative controls, respectively. Mequitazine (MQ), promethazine HCl (PM), chlorpromazine HCl (CP), QN, $NaH_2PO_4 \cdot 2H_2O$, $Na_2HPO_4 \cdot 12H_2O$, EM, midazolam, dimethyl sulfoxide (DMSO), *p*-nitrosodimethylaniline, imidazole, and nitroblue tetrazolium (NBT) were obtained from Wako Pure Chemical Industries (Osaka, Japan). Perphenazine (PP), fluphenazine 2HCl (FP), and thiolidazine HCl (TD) were purchased from Sigma-Aldrich Japan (Tokyo, Japan). Trifluoperazine 2HCl (TF) and prochlorperazine dimaleate (PC) were purchased from MP Biomedicals LCC (Santa Ana, California). A quartz reaction container for high-throughput ROS assay (Onoue *et al.*, 2008a) was constructed by Ozawa Science (Aichi, Japan). In this study, on the basis of previously reported photoreactivity and photosafety data (Onoue *et al.*, 2009), QN and EM were selected as positive and negative controls, respectively.

***UV spectral analysis.*** Chemicals were dissolved in 20mM sodium phosphate buffer (NaPB, pH 7.4) at a final concentration of 20μM. UV/VIS absorption spectra were recorded with a Hitachi U-2010 spectrophotometer (Hitachi High-Technologies Corporation, Tokyo, Japan) interfaced to a PC for data processing (software: Spectra Manager). A spectrofluorimeter quartz cell with 10mm pathlength was employed.

***Irradiation.*** The ROS assays were conducted using Atlas Suntest CPS plus (Atlas Material Technology LLC, Chicago, Illinois) equipped with a xenon arc lamp (1500W). A UV special filter was installed to adapt the spectrum of the artificial light source to that of natural daylight, and the Atlas Suntest CPS series had a high irradiance capability that met CIE85/1989 daylight simulation requirements (Supplementary Figure 1). The irradiation test was carried out for 1 h at 25°C with an irradiance of ca. 2.0 mW/cm$^2$ (7.2 J/cm$^2$) as determined by the calibrated UVA detector Dr Hönle no. 0037 (Dr Hönle, München, Germany).

***ROS assay procedure.*** ROS assay was carried out to detect both singlet oxygen and superoxide generated from photoirradiated chemicals according to the validated protocol with minor modification (Onoue *et al.*, 2013). Briefly, singlet oxygen was measured in an aqueous solution by spectrophotometrically monitoring the bleaching of *p*-nitrosodimethylaniline at 440nm using imidazole as a selective acceptor of singlet oxygen. Samples, containing the tested chemical (200μM), *p*-nitrosodimethylaniline (50μM), and imidazole (50μM) in 20mM NaPB (pH 7.4), were mixed in a tube. Two-hundred microliters of the sample was transferred into a well of a plastic 96-well plate (Asahi Glass Co., Ltd., Tokyo, Japan; code number: 3881-096; clear, untreated, flat bottomed) and checked for precipitation before light exposure. The plate was subjected to measurement of absorbance at 440nm using a SAFIRE microplate spectrophotometer (TECAN, Mannedorf, Switzerland). The plate was fixed in a quartz reaction container with a quartz cover and then irradiated with simulated sunlight for 1 h. After agitation on a plate shaker, the UV absorbance at 440nm was measured. For the determination of superoxide, samples containing the tested chemical (200μM) and NBT (50μM) in 20mM NaPB were irradiated with simulated sunlight for 1 h, and the reduction in NBT was measured by the increase in absorbance at 560nm in the same manner as the singlet oxygen determination.

***Cassette-dosing pharmacokinetic study.*** Male Sprague Dawley rats at 10–11 weeks of age (ca. 280–330g, body weight) were purchased from SLC Inc. (Hamamatsu, Japan), housed in the laboratory with free access to food and water, and maintained on a 12-h dark/light cycle in a room with controlled temperature (24±1°C) and humidity (55±5%). Rats ($n$ = 4) were fasted for approximately 18h before drug administration and received a cocktail solution containing all 8 PTZs orally (5mg/kg each). In general, the cassette-dosing approach is used in a low-dose level to reduce the risk of drug-drug interation (Smith *et al.*, 2007). In the preliminary study, at the dose of 1 mg/kg or lower, pharmacokinetic characterization of some PTZs was challenging because of very low systemic exposure. So, the nominal dose in this study was 5 mg/kg for each PTZ. All the procedures used in this study were conducted according to the guidelines approved by the Institutional Animal Care and Ethical Committee of the University of Shizuoka.

***Plasma concentration of PTZs after oral coadministration.*** All PTZs (5mg/kg each) were dissolved in ca. 1 ml of 0.1M acetic acid/sodium acetic acid buffer (pH 4.8) containing 0.05% Tween 20, and the mixture solution was administered orally. Blood samples (approximately 200 μl) were collected from the tail vein at the indicated times (0.25, 0.5, 1, 2, 4, 6, 10, 24, 48, and 72h) after oral coadministration of PTZs. Plasma obtained by centrifugation (10000 × g, 10min, 4°C) was deproteinized by the addition of acetonitrile. The mixture was mixed for a few seconds and centrifuged (3000rpm, 5min, 4°C). The supernatants were filtered, and 50% acetonitrile solution including midazolam (20 μg/ml), an internal standard, was added to them (supernatant:midazolam = 9:1) for UPLC analysis.

***Tissue deposition of PTZs after oral coadministration.*** At 4.5h after oral coadministration of PTZs, rats were humanely killed by taking blood from the descending aorta under temporary anesthesia with diethyl ether, and the tissues were then perfused with cold saline from the aorta. The skin and eyes were

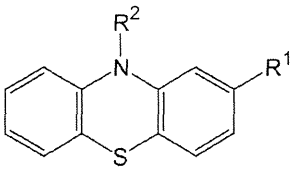

| PTZs | CAS No. | Clog $P^a$ | $R^1$ | $R^2$ |
|---|---|---|---|---|
| *Non-halogenated group* | | | | |
| Mequitazine (MQ) | 88598-74-7 | 4.91 | −H | 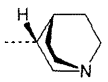 |
| Promethazine HCl (PM) | 58-33-3 | 4.60 | −H | 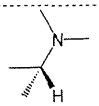 |
| Thioridazine HCl (TD) | 130-61-0 | 6.20 | $-SCH_3$ | 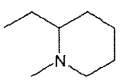 |
| *Fluorinated group* | | | | |
| Fluphenazine 2HCl (FP) | 146-56-5 | 4.32 | $-CF_3$ | 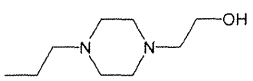 |
| Trifluoperazine 2HCl (TF) | 440-17-5 | 4.89 | $-CF_3$ | 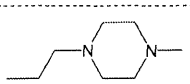 |
| *Chlorinated group* | | | | |
| Chlorpromazine HCl (CP) | 69-09-0 | 5.50 | −Cl | 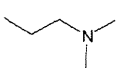 |
| Perphenazine (PP) | 58-39-9 | 4.01 | −Cl | 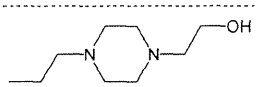 |
| Prochlorperazine dimaleate (PC) | 84-02-6 | 4.58 | −Cl | 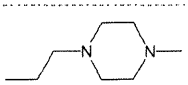 |

**FIG. 1.** Chemical structures of PTZs. [a]Calculated on ChemBioDraw Ultra 13.0 software. Abbreviation: PTZ, phenothiazine.

dissected, and the tissues were minced with scissors and homogenized in a Physcotron (Microtech Co., Ltd., Chiba, Japan) in 4 ml of acetonitrile. After shaking for 10 min and sonication for 10 min, the mixtures were centrifuged (3000 rpm, 10 min). Extraction was repeated twice with acetonitrile, and the supernatants were pooled. The collected eluents were pooled with acetonitrile extracts, and the samples were evaporated to dryness under a gentle stream of nitrogen at 40°C. The residues were dissolved in 50% acetonitrile including midazolam (20 μg/ml) as an internal standard for UPLC analysis. The tissue to plasma concentration ratio ($K_p$ value) was calculated as the ratio of the tissue concentration of unchanged drug to the plasma concentration.

***UPLC analysis.*** The concentrations of PTZs in rat tissues and plasma were determined by UPLC/ESI-MS analysis. The UPLC/ESI-MS system consisted of a Waters Acquity UPLC system (Waters, Milford, Massachusetts), which included a binary solvent manager, a sample manager, a column compartment, and a Micromass SQ detector connected with Waters Masslynx v 4.1. A Waters Acquity UPLC BEH C18 (particle size: 1.7 μm, column size: ϕ2.1×50 mm; Waters) was used, and the column temperature was maintained at 40°C. The standards and samples were separated using a gradient mobile phase consisting of Milli-Q containing 0.1% formic acid (A) and acetonitrile (B). The gradient conditions of the mobile phase were 0–1.0 min, 50% B; 1.0–4 min, 50%–95% B (linear gradient curve); 4–5 min, 95% B; and 5–6 min, 50% B, and the flow rate was set at 0.25 ml/min. Analysis was carried out using selected ion recording (SIR) for specific m/z 323.5 for MQ $[M+H]^+$, 285.4 for PM $[M+H]^+$, 371.6 for TD $[M+H]^+$, 438.5 for FP $[M+H]^+$, 408.5 for TF $[M+H]^+$, 319.8 for CP $[M+H]^+$, 404.9 for PP $[M+H]^+$, 374.9 for PC $[M+H]^+$, and 326.8 for midazolam, an internal standard, $[M+H]^+$. Peaks for MQ, PM, TD, FP, TF, CP, PP, PC, and midazolam were detected at retention times of 1.81, 1.38, 2.49, 2.22, 2.73, 1.93, 1.81, 2.21 and 1.86 min, respectively. The newly developed UPLC/ESI-MS method for determination of PTZs was validated in terms of linearity, accuracy, and precision according to International Conference on Harmonization of Technical Requirements for Registration of Pharmaceuticals for Human Use (ICH) guidelines "Q2B Validation of Analytical Procedures: Methodology." The pharmacokinetic parameters for PTZs were calculated by means of noncompartmental methods using the WinNonlin program (Ver. 4.1, Pharsight Corporation, Mountain View, California).

*In vivo* ***phototoxicity testing.*** Rats ($n$ = 4) were anesthetized using pentobarbital (30 mg/kg), and then the hair on the abdomen was shaved (5×5 cm). In the previous study, phototoxic dose of some PTZs in mice was found to be

80 mg/kg or higher (Ljunggren and Möller, 1977), so the dose of PTZs in this study was tentatively set to 100 mg/kg. Each PTZ or control (QN and EM) at the dose of 100 mg/kg was orally administered to rats ($n$ = 4 for each group) after awaking from anesthesia, and 3 h later, the rats were irradiated individually by black light (FL15BL-B, Panasonic, Tokyo, Japan) as UVA light source (Supplementary Figure 1) with an irradiance of ca. 2.7 mW/cm$^2$ for ca. 3 h until the UVA irradiance level reached 30 J/cm$^2$. Because UVB light is highly cytotoxic, UVA light source was employed for *in vivo* phototoxicity testing. During the UVA irradiation, rats were restrained on a sunbed for ensuring a uniform irradiation of their abdomen, and nonirradiated animals were kept in their housing cages under light protection. UV intensity was monitored using the calibrated UVA detector Dr Hönle no. 0037 (Dr Hönle). A colorimeter equipped with a data processor (NF333, Nippon Denshoku, Tokyo, Japan) was used as a measure of skin color. The instrument records 3-dimensional color reflectance, the so-called $L^*a^*b^*$ system, as recommended by the Commission Internationale de l'Eclairage (CIE). The luminance ($L^*$) gives the relative brightness ranging from total black ($L^* = 0$) to total white ($L^* = 100$). The hue ($a^*$) axis represents the balance between red (positive values up to 100) and green (negative values up to −100), and the chroma ($b^*$) axis represents the balance between yellow (positive values up to 100) and blue (negative values up to −100). The differences in skin color ($\Delta E$) between nonirradiated and irradiated groups were described as follows (Piérard and Piérard-Franchimont, 1993; Westerhof *et al.*, 1986):

$$\Delta E = \sqrt{\left[\left(\Delta L^*\right)^2 + \left(\Delta a^*\right)^2 + \left(\Delta b^*\right)^2\right]}$$

***Matrix decision making for photosafety prediction.*** The matrix decision approach was applied to photosafety prediction of PTZs by combined use of photochemical and cassette-dosing pharmacokinetics data. The risk score (0–5) was tentatively assigned to UV absorption data, ROS generation, and skin/ocular distribution of PTZs as follows: (1) UV data (MEC value): **0**, < 1000; **1**, 1000 to < 1750; **2**, 1750 to < 2500; **3**, 2500 to < 3250; **4**, 3250 to < 4000; and **5**, ≥ 4000; (2) ROS data (higher level of singlet oxygen or superoxide): **0**, < 25 (singlet oxygen) and 20 (superoxide); **1**, 25 (singlet oxygen) or 20 (superoxide) to < 160; **2**, 160 to < 295; **3**, 295 to < 430; **4**, 430 to < 565; and **5**, ≥ 565; and (3) tissue distribution of PTZs (total amount in skin and eyes): **1**, < 350; **2**, 350 to < 700; **3**, 700 to < 1050; **4**, 1050 to < 1400; and **5**, ≥ 1400. Total risk scores were used for rank ordering of phototoxicity potential.

***Data analysis.*** For statistical comparisons, 1-way ANOVA with pairwise comparison by Fisher's least significant difference procedure was used. A $p$ value of less than .05 was considered significant for all analyses. Theoretical calculations of the lipophilicity as calculated log $P$ (Clog $P$) were performed by ChemBioDraw Ultra 13.0 (Cambridge Soft. Corp., Cambridge, Massachusetts) using chemical structure inputs.

## RESULTS

### *Photochemical Properties of PTZs*

In the early stage of phototoxicity, the absorption of sunlight, in particular UVA/B and VIS, can be a key trigger for the excitation of phototoxins, so the UV-absorbing property of a tested chemical would be an indicator of phototoxic potential (Henry *et al.*, 2009). Herein, UV spectral analysis was conducted for 8 PTZs, including (1) nonhalogenated group: MQ, PM, and TD, (2) fluorinated group: FP and TF, and (3) chlorinated group: CP, PP, and PC (Fig. 2A). All PTZs exhibited intense absorption in UVA and B regions with $\lambda_{max}$ values of 299–312 nm, and there was no absorption in the VIS region (data not shown). Molar extinction coefficients (MECs) of PTZs were calculated to be ca.

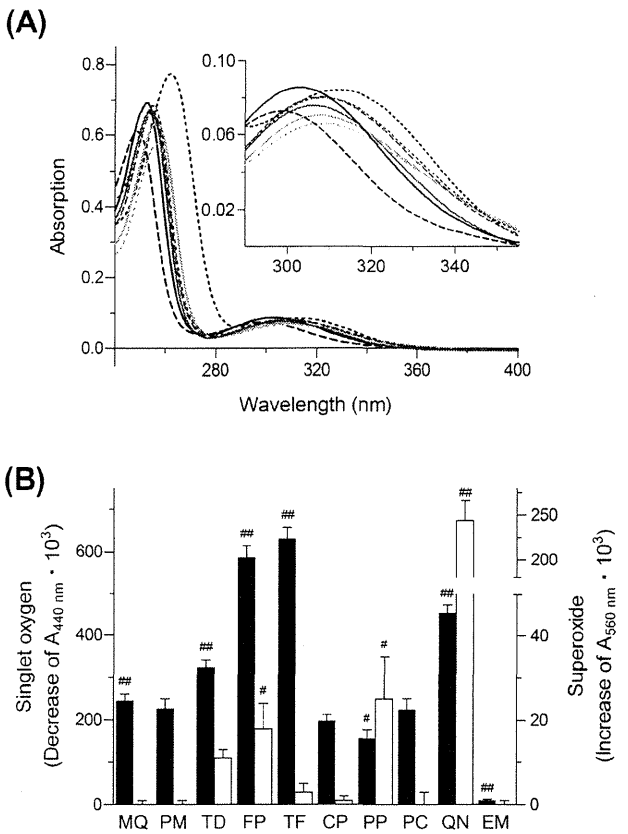


**FIG. 2.** Photochemical properties of PTZs. A, UV spectral patterns of PTZs (20μM) in 20mM NaPB (pH 7.4). Solid line, MQ; broken line, PM; dotted line, TD; green solid line, FP; green dotted line, TF; red solid line, CP; red broken line, PP; and red dotted line, PC. B, Generation of singlet oxygen (filled bars) and superoxide (open bars) from PTZs (200μM) exposed to simulated sunlight (2.0 mW/cm$^2$). QN as positive control and EM as negative control. Data represent mean ± SD of 3 experiments. $^{\#}p < .05$ and $^{\#\#}p < .01$ with respect to CP in each reactive oxygen species determination. Abbreviations: CP, chlorpromazine; EM, erythromycin; FP, fluphenazine; MQ, mequitazine; PC, prochlorperazine dimaleate; PM, promethazine HCl; PP, perphenazine; PTZ, phenothiazine; QN, quinine HCl; TD, thiolidazine HCl; TF, trifluoperazine.

3400–4400 M$^{-1}$cm$^{-1}$. Previously, Henry and coworkers suggested that chemicals with an MEC of less than 1000 M$^{-1}$cm$^{-1}$ were less of a phototoxic risk because this low level of light absorption was unlikely to prove harmful (Henry *et al.*, 2009). Using this tentative threshold, all PTZs can be identified to be photoreactive and potentially phototoxic.

For further photochemical characterization of PTZs, the ROS assay was applied to these chemicals (Fig. 2B), in which quinine, a typical phototoxin, and EM, a nonphototoxic drug, were also assessed for comparison. As observed previously (Onoue and Tsuda, 2006), significant generation of singlet oxygen and superoxide was observed for quinine under exposure to simulated sunlight, but not for EM. All photoirradiated PTZs tended to generate singlet oxygen through type II photochemical reaction. The type II photochemical reaction can be characterized as an energy transfer from excited

triplet photosensitizer to the oxygen, resulting in generation of excited singlet oxygen which might, in turn, participate in a lipid- and protein-membrane oxidation or induce DNA damage (Onoue *et al.*, 2009). In contrast, weak generation of superoxide was seen for only TD, FP, and PP. In particular, fluorinated PTZs were found to be potent ROS generators, and the order of ROS-generating ability was as follows: FP ≒ TF ≫ TD > MQ ≒ PM ≒ CP ≒ PC > PP. All PTZs were identified as photoreactive according to the previously defined threshold (singlet oxygen [$\Delta A_{440\ nm} \cdot 10^3$]: 25; superoxide [$\Delta A_{560\ nm} \cdot 10^3$]: 20) (Onoue *et al.*, 2008b, 2013). From these findings, taken together with MEC values, PTZs would be photoreactive, which raises concerns about their photosafety when they could be distributed to UV-exposed tissues.

*Pharmacokinetic Behaviors of PTZs*

Phototoxic skin responses typically appear in UV-exposed tissues such as skin and eyes; therefore, the specific distribution of PTZs to the skin and/or eyes could be a key consideration for their photosafety evaluation. In this study, cassette-dosing pharmacokinetic analysis was employed for screening purposes, offering high throughput and reduction of animal used. After oral cassette dosing of 8 PTZs (5 mg/kg each) in rats, the concentration-time curves in the plasma were obtained by UPLC/ESI-MS analysis (Fig. 3A), and the PK parameters were calculated from the data obtained (Table 1). After oral coadministration of PTZs, most PTZs showed gradual elevation of plasma levels with a $T_{max}$ of ca. 3–4.5 h, whereas apparent absorption of MQ was much slower, as evidenced by $T_{max}$ of 17 h. Systemic exposure of PTZs after coadministration was quite different with $C_{max}$ values of ca. 10–120 ng/ml, and the calculated $C_{max}$ of plasma PTZs was ranked as follows: FP > TF > TD > MQ ≒ PP ≒ PC > PM ≒ CP. There appeared to be a slow elimination phase for all PTZs with elimination rates of ca. 0.03–0.39 $h^{-1}$, and thus, PTZs may accumulate in light-exposed areas upon chronic dosing, resulting in an increased phototoxic risk.

Because most PTZs reached $C_{max}$ at ca. 4.5 h after oral coadministration, the distribution of PTZs to the light-exposed tissues (skin and eyes) was monitored at this time period for photosafety prediction (Fig. 3B). Most PTZs were found to be delivered to the light-exposed areas, in particular, skin, in which major phototoxic responses would occur. FP exhibited high distribution to skin (637 ng/g tissue) and eyes (548 ng/g tissue), with $K_p$ values of 5.6 and 4.8 ml/g tissue, respectively, and the data could be consistent with high systemic exposure of FP with a $C_{max}$ value of ca. 120 ng/ml. Interestingly, PP exceeded FP in skin and ocular distribution, the $K_p$ value of which was ca. 4-fold higher than that of FP. In spite of its high systemic exposure, of all PTZs tested, the lowest concentrations of TD were observed in both skin (72 ng/g tissue) and eyes (40 ng/g tissue). In contrast, relatively high tissue concentrations of PM were seen in skin (336 ng/g tissue) and eyes (162 ng/g tissue) although there appeared to be the lowest systemic exposure for PM.

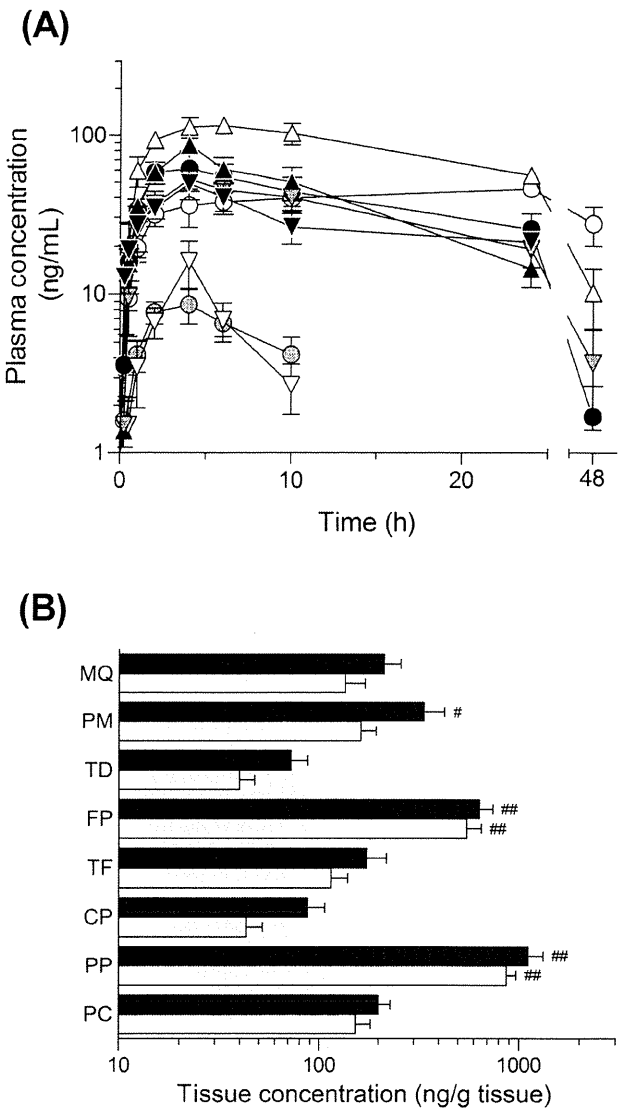


**FIG. 3.** Pharmacokinetic characteristics of PTZs in rats. A, Plasma concentrations of PTZs in rats after oral cassette dosing of 8 PTZs (5 mg/kg each). ○, MQ; , PM; ● TD; △, FP; ▲, TF; ▼, CP; , PP; ▼, PC. Data represent mean ± SE of 4 experiments. B. Deposition of PTZs in skin (filled bars) and eyes (open bars) at 4.5 h after oral cassette dosing of 8 PTZs (5 mg/kg each). Data represent mean ± SE of 4 experiments. $^{\#}p < .05$ and $^{\#\#}p < .01$ with respect to TD. Abbreviations: CP, chlorpromazine; EM, erythromycin; FP, fluphenazine; MQ, mequitazine; PC, prochlorperazine dimaleate; PM, promethazine HCl; PP, perphenazine; PTZ, phenothiazine; QN, quinine HCl; TD, thiolidazine HCl; TF, trifluoperazine.

Thus, the order of skin and ocular distribution was as follows: PP ≫ FP > PM > MQ ≒ PC ≒ TF > CP ≒ TD. On the basis of the distribution to the light-exposed areas, PP and FP would be more likely to cause phototoxic reactions than the other PTZs if they could undergo photochemical activation there. In contrast, TD and CP might be less phototoxic in terms of their lower concentrations in skin and eyes.

**TABLE 1**
**Pharmacokinetic Parameters of PTZs After Oral Cassette Dosing**

| | $C_{max}$ (ng/ml) | $T_{max}$ (h) | $K_{el}$ ($h^{-1}$) | $AUC_{0-inf}$ (ng·h/ml) |
|---|---|---|---|---|
| MQ | 52.3±3.6 | 17.0±4.0 | 0.033±0.019 | 5395±473 |
| PM | 9.8±1.5 | 3.0±0.6 | 0.13±0.046 | 301±36 |
| TD | 66.1±14.8 | 4.0±0.8 | 0.044±0.026 | 1604±308 |
| FP | 119.8±12.3 | 4.0±0.8 | 0.030±0.013 | 4310±304 |
| TF | 75.6±13.4 | 4.0±0.8 | 0.088±0.026 | 1415±191 |
| CP | 13.5±4.6 | 3.3±0.8 | 0.39±0.13 | 109±30 |
| PP | 53.4±3.2 | 4.5±0.5 | 0.045±0.012 | 1325±170 |
| PC | 52.7±8.5 | 3.3±0.8 | 0.054±0.034 | 985±292 |

*Note.* $C_{max}$, maximum concentration; $T_{max}$, time to maximum concentration; $K_{el}$, apparent elimination rate constant; $AUC_{0-inf}$, area under the curve of blood concentration vs time from $t = 0$ to $t = \infty$ after administration. Values are expressed as mean ± SE of 4 experiments.

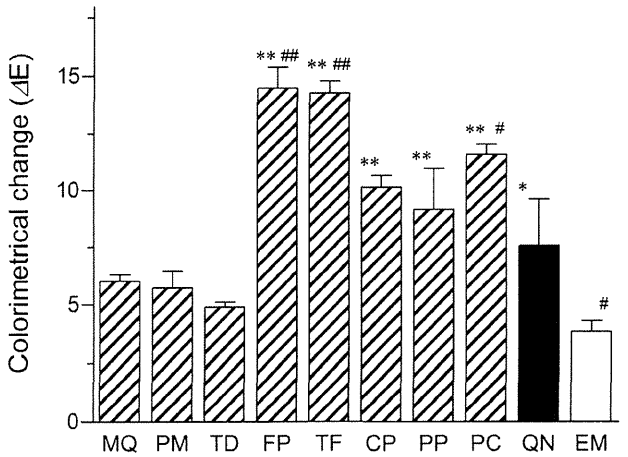


**FIG. 4.** Colorimetrical evaluation of PTZ-induced phototoxic skin response. Differences in skin color ($\Delta E$) between irradiated and nonirradiated rats treated with each drug (100 mg/kg, PO) were calculated on the basis of $L^*$, $a^*$, and $b^*$ values. QN as positive control and EM as negative control. Data represent mean ± SE of 4 experiments. $^*p < .05$ and $^{**}p < .01$ with respect to EM-treated group; $^{\#}p < .05$ and $^{\#\#}p < .01$ with respect to QN-treated group. Abbreviations: CP, chlorpromazine; EM, erythromycin; FP, fluphenazine; MQ, mequitazine; PC, prochlorperazine dimaleate; PM, promethazine HCl; PP, perphenazine; PTZ, phenothiazine; QN, quinine HCl; TD, thiolidazine HCl; TF, trifluoperazine.

Because lipophilicity has been thought as a dominant determining factor in the distribution of basic drugs in the tissues (Abraham and Ibrahim, 2007), Clog *P* values of PTZs were also calculated as indicator of their lipophilicity (Fig. 1). The Clog *P* values of PTZs were in the range of 4.0–6.2, and overall values of the Clog *P* were not well correlated with the distribution of PTZs to the light-exposed tissues as well as oral absorption. From these findings, it might be challenging to predict tissue distribution of PTZs only by the lipophilicity and related parameters, so *in vivo* study would be still needed to provide reliable pharmacokinetic data.

*In vivo Phototoxicity of PTZs*

To clarify the *in vivo* photosafety of PTZs, phototoxic skin responses were monitored in rats because skin is a major site of drug-induced phototoxicity. From previous investigations, CP and its related compounds exhibited significant phototoxic responses at a dose of 80 mg/kg or higher in mice exposed to UVA (Ljunggren and Möller, 1977); therefore, in this study, after oral administration of each PTZ or positive/negative control at a dose of 100 mg/kg, *in vivo* cutaneous inflammation was examined in rats exposed to UVA (Fig. 4). The transition in skin color was determined using a colorimeter with the $L^*a^*b^*$ system, where $L^*$ represents the brightness of shade and $a^*$ and $b^*$ represent the amount of red-green and yellow-blue color, respectively. In the colorimetrical evaluation on the surface of the skin, the $\Delta E$ values of nonirradiated rats treated with quinine (100 mg/kg), a positive control, were not significantly different from those of nonirradiated rats in the vehicle group (data not shown). In contrast, irradiated rats with quinine exhibited an increase of $\Delta E$ values by 7.6±2.1 compared with the nonirradiated group, owing to the increase of $b^*$ values in the UV-exposed group as observed in a previous study (Nose and Tsurumi, 1993). As observed for quinine, the $\Delta E$ values of UV-exposed rats in all PTZ-treated groups were much higher than those of nonirradiated rats in corresponding groups. In particular, after exposure to UV, orally administered FP (100 mg/kg) led to significant colorimetrical changes on the surface of the skin, with increases of $L^*$($\Delta L^*$: 11.4±0.7) and $b^*$($\Delta b^*$: 3.4±0.7) and a decrease of $a^*$($\Delta a^*$: −8.2±0.9). According to the $\Delta E$ values for TF and PC, they also caused significantly higher phototoxic skin responses compared with quinine ($p < .05$). In contrast, UV-exposed rats with nonhalogenated PTZs (MQ, PM, and TD; 100 mg/kg) exhibited lower $\Delta E$ values than the UV-exposed rats in other groups in the present evaluation, suggesting less phototoxicity. As observed in this study, phototoxicity of TD was negligible in previous photohemolysis testing (Eberlein-König *et al.*, 1997); however, photopatch testing demonstrated that TD induced immediate and delayed photodynamic erythema in humans (Takiwaki *et al.*, 2006). Thus, phototoxicity of TD may be a matter of controversy, and experimental and species differences may be the causes of the data discrepancy. In rats, the observed phototoxic responses of PTZs can be rated as follows: FP ≒ TF > PC > PP ≒ CP ≫ MQ ≒ PM ≒ TD. Thus, the phototoxicity of PTZs in rats seemed to depend on the chemical series, and the halogenated and chlorinated PTZs were deduced to be highly phototoxic.

## DISCUSSION

In this study, simplified prediction of the photosafety of PTZs was attempted by combined use of their photochemical and pharmacokinetic data. As photochemical testing, UV spectral analysis and ROS assay were carried out, in which all PTZs could be identified as photoreactive in the following order: FP ≒ TF ≫ TD > MQ ≒ PM ≒ CP ≒ PC > PP. According to the

cassette-dosing pharmacokinetic study using UPLC/ESI-MS, most PTZs exhibited high distribution to the skin and eyes in the following order: PP ≫ FP > PM > MQ ≒ PC ≒ TF > CP ≒ TD. To integrate these data for photosafety prediction, a decision matrix was built upon *in vitro* and *in vivo* experimental outcomes (Table 2).

In general, the decision matrix can be a summarized schematic model of qualitative or quantitative scores, allowing systematic identification, analysis, and evaluation of complicated sets of experimental outcomes (Seto *et al.*, 2011). In the present matrix decision making, high scoring in both photochemical and pharmacokinetic behavior might be indicative of high phototoxic potential; however, when either of the two is at a low level, the tested chemical can be identified as mildly or less phototoxic. With respect to the photochemical data, the UV-absorbing and ROS-generating properties were employed to rate the PTZs. UV spectral analysis can provide information on the photoexcitability of tested chemicals on the basis of the first law of photochemistry, and the UV absorption would be a key trigger for subsequent photochemical reactions. According to the MEC-based approach proposed by Henry and coworkers (2009), all PTZs tested here could be identified to be photoreactive and potentially phototoxic because their MEC values were found to be over $1000\,M^{-1}cm^{-1}$. However, the actual photoreactivity of chemicals, possibly leading to a phototoxic reaction, is unclear because some excited chemicals release photon energy via the emission of fluorescence, phosphorescence, and heat (Onoue and Tsuda, 2006). In a previous study, UV absorption of chemicals did not always correlate with their phototoxic potential directly (Onoue *et al.*, 2008a), so some compounds might be falsely predicted to be phototoxic or nonphototoxic according to UV spectral analysis alone. Herein, further use of the ROS data would be important for exact rating because the obtained ROS data could suggest the photochemical reactivity of the tested chemical directly. However, the ROS assay has two major assay limitations: (1) poor applicability to chemicals with low solubility in water and (2) spectral interference on ROS determination in chemicals with potent absorption at 440 and 560 nm (Onoue *et al.*, 2013). Therefore, combination use of UV and ROS data would provide reliable photochemical information on tested chemicals. In this study, both FP and TF were deduced to be highly photoreactive because of potent UV absorption and ROS generation, and order of photoreactivity was deduced as follows: fluorinated PTZs ≫ nonhalogenated PTZs ≥ chlorinated PTZs. With respect to the pharmacokinetic data, distribution of each PTZ to skin and eyes was employed as important pharmacokinetic profile for the decision matrix. As described in ICH S10 draft guideline (ICH, 2013), photoreactive chemicals having longer residence times in light-exposed tissues or with higher tissue to plasma concentration ratios are more likely to produce a phototoxic tissue reaction than compounds with shorter residence times or lower tissue to plasma ratios. However, even though the tested chemicals exhibited high skin and ocular deposition, they might be less phototoxic as long as their photoreactivity is highly limited. Thus, strategic use of photobiochemical and pharmacokinetic data might allow reliable photosafety evaluation. As shown in Table 2, risk scores were assigned to the UV data, ROS generation,

**TABLE 2**
**Decision Matrix for Photosafety Evaluation**

| | Nonhalogenated Group | | | Fluorinated Group | | Chlorinated Group | | |
|---|---|---|---|---|---|---|---|---|
| | MQ | PM | TD | FP | TF | CP | PP | PC |
| Photochemical properties | | | | | | | | |
| UV absorption, $\lambda_{max}/\varepsilon$ ($M^{-1}cm^{-1}$) | 302 nm/4350 | 299 nm/3700 | 312 nm/4250 | 308 nm/3550 | 307 nm/3350 | 306 nm/3850 | 308 nm/4050 | 309 nm/4050 |
| | [5][a] | [4] | [5] | [4] | [4] | [4] | [5] | [5] |
| ROS assay[b] $^1O_2$ ($\Delta A_{440nm} \times 10^3$) | 245 | 226 | 323 | 586 | 630 | 197 | 156 | 224 |
| $O_2^-$ ($\Delta A_{560nm} \times 10^3$) | 0 | 0 | 11 | 18 | 3 | 1 | 25 | 0 |
| | [2] | [2] | [2] | [4] | [5] | [2] | [1] | [2] |
| Distribution to UV-exposed tissues | | | | | | | | |
| Skin (ng/g tissue)[c] | 211.4 | 336.3 | 72.3 | 636.5 | 173.3 | 87.5 | 1109.3 | 199.7 |
| | (4.2)[d] | (41.5) | (1.2) | (5.6) | (2.5) | (8.1) | (21.9) | (4.3) |
| Eyes (ng/g tissue)[c] | 135.1 | 162.0 | 39.8 | 547.5 | 114.8 | 43.1 | 865.9 | 152.9 |
| | (2.7) | (20.0) | (0.7) | (4.8) | (1.7) | (4.0) | (17.1) | (3.3) |
| | [1] | [2] | [1] | [4] | [1] | [1] | [5] | [2] |
| Total score | 8 | 8 | 8 | 12 | 10 | 7 | 11 | 9 |

*Note.* White cells, risk score 0–1; gray cells, 2–3; and black cells, 4–5.
[a]Risk scores in parentheses.
[b]ROS data for PTZs at a concentration of 200 μM.
[c]Tissue concentration of PTZs at 4.5 h after oral cassette dosing.
[d]$K_p$ values (ml/g tissue) in parentheses.

**TABLE 3**
**Summary of Outcomes From Photosafety Testing on PTZs**

| | Obtained Data/Prediction |
|---|---|
| Experimental data | |
| Photoreactivity (UV, ROS) | FP ≒ TF ≫ TD > MQ ≒ PM ≒ CP ≒ PC > PP |
| Skin/ocular distribution | PP ≫ FP > PM > MQ ≒ PC ≒ TF > CP ≒ TD |
| *In vivo* phototoxicity | FP ≒ TF > PC > PP ≒ CP ≫ MQ ≒ PM ≒ TD |
| Matrix decision | FP > PP > TF > PC > MQ ≒ PM ≒ TD > CP |
| Conclusion | Fluorinated PTZs > Chlorinated > Nonhalogenated |

*Note.* White cells, nonhalogenated PTZs; gray cells, chlorinated PTZs; and black cells, fluorinated PTZs.

and tissue distribution of PTZs to the UV-exposed tissues in accordance with tentatively defined criteria. On the basis of the phototoxic evaluation using the decision matrix, the sensitive photoreactivity (both risk scores for UV and ROS: 4) and high concentrations of FP in the light-exposed area (risk score: 4) were predictive of the most potent phototoxic risk. There also seemed to be potent phototoxic potential in TF (total risk score: 10) and PP (total risk score: 11) because of potent ROS generation or high skin and ocular deposition. In particular, TF has the highest ability to generate singlet oxygen (risk score: 5) under light exposure, thereby leading to potent phototoxic responses when TF could accumulate in the skin and/or eyes. Compared with the present results on FP, TF, and PP, those on PC, MQ, PM, and TD were indicative of less photochemical reactivity and/or deposition in light-exposed area; therefore, PC, MQ, PM, and TD might have less phototoxic risk (total risk score: 8–9). Photoirradiated CP exhibited generation of singlet oxygen; however, the low distribution to skin and eyes (risk score: 1) suggested that CP might have limited phototoxic potential (total risk score: 7). On the basis of these data, phototoxic risk of PTZs can be deduced in the following order: FP > PP > TF > PC > MQ ≒ PM ≒ TD > CP (Table 3).

According to the results from *in vivo* phototoxicity testing, most tested PTZs were found to be phototoxic in rats, and the order of phototoxic potential was summarized as follows: FP ≒ TF > PC > PP ≒ CP ≫ MQ ≒ PM ≒ TD. There seemed to be a clear structure-phototoxicity relationship for the PTZs, suggesting the following tentative order of phototoxicity: fluorinated PTZs > chlorinated PTZs > nonhalogenated PTZs. The outcomes from the decision matrix approach were likely to be in agreement with the present observations, and there seemed to be few exceptions. In particular, satisfactory photosafety prediction can be made on FP, TF, MQ, PM, and TD, suggesting high predictability of the present photosafety assessment using photochemical and pharmacokinetic data. In contrast, the new screening system gave severe false predictions on CP. Experimental and clinical observations on CP demonstrated its high phototoxicity (Ljunggren and Möller, 1977), as observed in our *in vivo* phototoxicity testing. CP showed high ROS generation but limited skin and ocular deposition, and it was thereby predicted to be less phototoxic. Interestingly, for some drugs, their metabolites have been recognized as major effectors in phototoxic responses (Ferguson *et al.*, 1985; Ljunggren and Möller, 1977). Orally taken CP would undergo severe metabolism, such as N-demethylation by CYP1A2 and CYP3A4 and 7-hydroxylation by CYP2D6 (Wójcikowski *et al.*, 2010), and demethylated CPs (desmethylchlorpromazine and didesmethylchlorpromazine) were found to be more phototoxic than CP itself (Ljunggren and Möller, 1977). Other metabolites of CP, including hydroxylated and sulfated metabolites, were also shown to be phototoxic but weaker than CP. From these previous findings, possible yield of phototoxic metabolites may be part of the reason for the false photosafety prediction of CP. There is also the probability that the photochemical reaction of compounds with ROS resulted in the yield of some toxic degradants. The study design for the present photosafety assessment focused on only parent drugs, possibly resulting in the limited prediction capacity. Therefore, there might be a future need to consider photochemical and/or pharmacokinetic profiles of major metabolites, and inclusion of these data in the decision matrix might allow more reliable photosafety evaluation.

Cassette dosing is a procedure for higher throughput screening in drug discovery to rapidly assess pharmacokinetics of large numbers of drug candidates. On the contrary, there are possible complications associated with the approach as the number of applied chemicals increases (Manitpisitkul and White, 2004). A major concern is the risk of drug-drug interactions after coadministration of multiple drugs, and the interaction would be attributable to competitive inhibition of drug-metabolizing enzymes, transporter, or plasma protein binding. Thus, pharmacokinetic data acquired from cassette dosing might be a little different from those indicated by the discrete dosing of individual chemicals, and this might lead to false positive/negative predictions in the photosafety evaluation. However, the cassette-dosing approach would be advantageous in terms of high throughput and reduction of labor, killed animals, and other research resources when used as a screen, especially to rank order drug candidates (White and Manitpisitkul, 2001). They might outweigh the disadvantages of cassette-dosing approach at least for screening purpose because a large number of new drug candidates have to be examined in an early phase of drug discovery. To minimize the potential for pharmacokinetic interactions, Smith and coworkers suggested that the lower doses should be used, and the total number of coadministered chemicals should be small (< 5) (Smith *et al.*, 2007). In addition, prescreening for potent CYP inhibitors and their exclusion might avoid pharmacokinetic interactions.

Interest in the photosafety of chemicals would increase further in both regulatory sciences and drug discovery to produce new drug candidates with high photosafety margin. From the present findings, with few exceptions, *in vivo* photosafety of PTZs could be effectively evaluated by combined use of photochemical and

cassette-dosing pharmacokinetic experiments. Recently, regulatory agencies have recommended the implementation of the 3Rs principle (refinement, reduction, and replacement), and the newly developed photosafety prediction system would meet this requirement in the sense of reduction and replacement. Although there would still be a need for further investigation to verify the applicability of the present simplified screening system to other chemical series, the present decision matrix approach might provide reliable photosafety assessments and aid productive research and the development of new pharmaceutics.

## SUPPLEMENTARY DATA

Supplementary data are available online at http://toxsci.oxfordjournals.org/.

## CONFLICT OF INTEREST

None of the authors has any conflicts of interest associated with this study.

## FUNDING

Health Labour Sciences Research Grant from The Ministry of Health, Labour and Welfare, Japan.

## REFERENCES

Abraham, M. H., and Ibrahim, A. (2007). Blood or plasma to skin distribution of drugs: A linear free energy analysis. *Int. J. Pharm.* **329,** 129–134.

Chignell, C. F., Motten, A. G., and Buettner, G. R. (1985). Photoinduced free radicals from chlorpromazine and related phenothiazines: Relationship to phenothiazine-induced photosensitization. *Environ. Health Perspect.* **64,** 103–110.

Corbett, M. F., Davis, A., and Magnus, I. A. (1978). Personnel radiation dosimetry in drug photosensitivity: Field study of patients on phenothiazine therapy. *Br. J. Dermatol.* **98,** 39–46.

Eberlein-König, B., Bindl, A., and Przybilla, B. (1997). Phototoxic properties of neuroleptic drugs. *Dermatology* **194,** 131–135.

EMEA/CPMP (2002). *Note for Guidance on Photosafety Testing*, CPMP/SWP/398/01. EMEA/CPMP.

FDA/CDER (2002). *Guidance for Industry, Photosafety Testing*. FDA/CDER.

Ferguson, J., Addo, H. A., Jones, S., Johnson, B. E., and Frain-Bell, W. (1985). A study of cutaneous photosensitivity induced by amiodarone. *Br. J. Dermatol.* **113,** 537–549.

Henry, B., Foti, C., and Alsante, K. (2009). Can light absorption and photostability data be used to assess the photosafety risks in patients for a new drug molecule? *J. Photochem. Photobiol. B.* **96,** 57–62.

ICH (2013). *ICH Guideline S10 Guidance on Photosafety Evaluation of Pharmaceuticals* (draft). ICH.

Ljunggren, B., and Möller, H. (1977). Phenothiazine phototoxicity: An experimental study on chlorpromazine and its metabolites. *J. Invest. Dermatol.* **68,** 313–317.

Manitpisitkul, P., and White, R. E. (2004). Whatever happened to cassette-dosing pharmacokinetics? *Drug Discov. Today* **9,** 652–658.

Miolo, G., Levorato, L., Gallocchio, F., Caffieri, S., Bastianon, C., Zanoni, R., and Reddi, E. (2006). In vitro phototoxicity of phenothiazines: Involvement of stable UVA photolysis products formed in aqueous medium. *Chem. Res. Toxicol.* **19,** 156–163.

Moore, D. E. (1998). Mechanisms of photosensitization by phototoxic drugs. *Mutat. Res.* **422,** 165–173.

Moore, D. E. (2002). Drug-induced cutaneous photosensitivity: Incidence, mechanism, prevention and management. *Drug Saf.* **25,** 345–372.

Nose, T., and Tsurumi, K. (1993). Pharmacological studies on cutaneous inflammation induced by ultraviolet irradiation (1): Quantification of erythema by reflectance colorimetry and correlation with cutaneous blood flow. *Jpn. J. Pharmacol.* **62,** 245–256.

OECD (2004). *OECD Guideline for Testing of Chemicals, 432, In Vitro 3T3 NRU Phototoxicity Test.*

Onoue, S., Hosoi, K., Wakuri, S., Iwase, Y., Yamamoto, T., Matsuoka, N., Nakamura, K., Toda, T., Takagi, H., Osaki, N., *et al.* (2013). Establishment and intra-/inter-laboratory validation of a standard protocol of reactive oxygen species assay for chemical photosafety evaluation. *J. Appl. Toxicol.* **33,** 1241–1250.

Onoue, S., Igarashi, N., Yamada, S., and Tsuda, Y. (2008a). High-throughput reactive oxygen species (ROS) assay: An enabling technology for screening the phototoxic potential of pharmaceutical substances. *J. Pharm. Biomed. Anal.* **46,** 187–193.

Onoue, S., Kawamura, K., Igarashi, N., Zhou, Y., Fujikawa, M., Yamada, H., Tsuda, Y., Seto, Y., and Yamada, S. (2008b). Reactive oxygen species assay-based risk assessment of drug-induced phototoxicity: Classification criteria and application to drug candidates. *J. Pharm. Biomed. Anal.* **47,** 967–972.

Onoue, S., Seto, Y., Gandy, G., and Yamada, S. (2009). Drug-induced phototoxicity: an early in vitro identification of phototoxic potential of new drug entities in drug discovery and development. *Curr. Drug Saf.* **4,** 123–136.

Onoue, S., and Tsuda, Y. (2006). Analytical studies on the prediction of photosensitive/phototoxic potential of pharmaceutical substances. *Pharm. Res.* **23,** 156–164.

Piérard, G. E., and Piérard-Franchimont, C. (1993). Dihydroxyacetone test as a substitute for the dansyl chloride test. *Dermatology* **186,** 133–137.

Seto, Y., Hosoi, K., Takagi, H., Nakamura, K., Kojima, H., Yamada, S., and Onoue, S. (2012). Exploratory and regulatory assessments on photosafety of new drug entities. *Curr. Drug Saf.* **7,** 140–148.

Seto, Y., Inoue, R., Ochi, M., Gandy, G., Yamada, S., and Onoue, S. (2011). Combined use of in vitro phototoxic assessments and cassette dosing pharmacokinetic study for phototoxicity characterization of fluoroquinolones. *AAPS J.* **13,** 482–492.

Smith, N. F., Raynaud, F. I., and Workman, P. (2007). The application of cassette dosing for pharmacokinetic screening in small-molecule cancer drug discovery. *Mol. Cancer Ther.* **6,** 428–440.

Takiwaki, H., Tsuchiya, K., Fujita, M., and Miyaoka, Y. (2006). Thioridazine induces immediate and delayed erythema in photopatch test. *Photochem. Photobiol.* **82,** 523–526.

Viola, G., and Dall'Acqua, F. (2006). Photosensitization of biomolecules by phenothiazine derivatives. *Curr. Drug Targets* **7,** 1135–1154.

Westerhof, W., van Hasselt, B. A., and Kammeijer, A. (1986). Quantification of UV-induced erythema with a portable computer controlled chromameter. *Photodermatol.* **3,** 310–314.

White, R. E., and Manitpisitkul, P. (2001). Pharmacokinetic theory of cassette dosing in drug discovery screening. *Drug Metab. Dispos.* **29,** 957–966.

Wójcikowski, J., Boksa, J., and Daniel, W. A. (2010). Main contribution of the cytochrome P450 isoenzyme 1A2 (CYP1A2) to N-demethylation and 5-sulfoxidation of the phenothiazine neuroleptic chlorpromazine in human liver–A comparison with other phenothiazines. *Biochem. Pharmacol.* **80,** 1252–1259.